
# Additive manufacturing of foamed structures

Master degree in Product Design Engineering

Abhishek Mistry

Leiria, July of 2022

escola superior de tecnologia e gestão
instituto politécnico de leiria

# Additive manufacturing of foamed structures

Master degree in Product Design Engineering

Abhishek Mistry

Dissertation/Project Report under the supervision of Doctor Fábio Jorge Pereira Simões, and Doctor Artur Jorge dos Santos Mateus.

Leiria, July of 2022

# Originality and Copyright

This dissertation/project report is original, made only for this purpose, and all authors whose studies and publications were used to complete it are duly acknowledged.

# Acknowledgments

This research work was performed as a conclusion of the master's program in Product Design Engineering at the School of Technology and Management, Polytechnic of Leiria, and the experimental tests were made at CDRSP.

I want to thank my supervisors, Prof. Fábio Jorge Pereira Simões and Prof. Artur Mateus, for their encouragement, patience, and continual support of my master's thesis.

I also want to thank the CDRSP family and all the technical team there for their assistance in the lab, especially Prof. Artur Mateus, who has given me ongoing support and insights into the innovative 3D printing of bubble-based Additive Manufacturing process.

# Abstract

The major aim of this work was to develop an additive manufacturing method for obtaining foamed structures. There is limited research to understand the properties of the materials and the technology used to make foamed parts directly by additive methods. Initially a process was developed that involved using a syringe and DLP (Digital Light Processing) to create bubbles inside the photo-polymer resin. However, the results were unappealing, so upon further literature review, inspiration was found in a research paper in which the authors used an SLA (stereolithography) printer to create foamed parts by means of a polymer resin blended with a foaming agent that caused the part to expand after printing. Additionally, this research includes a thorough investigation of the mechanical characteristics of foams with various infill structures.

**Keywords:** 3D printing, additive manufacturing, DLP, SLA, photo-polymer resin

# Contents

# List of Figures

# List of Tables

# 1. Introduction

This project aims to develop a method for building foam structures by means of additive manufacturing. In the literature, design and building approaches have been explored but there are limited examples of foam parts built directly by additive manufacturing. Two approaches were presented to address this problem. The first approach devised entailed producing foam cells by injecting air into a photo-polymerizable resin using a syringe and then using DLP (Digital Light Processing) to cure the resulting foamed structure. However, the results were unappealing, so it was decided to explore a solution found in literature in which the authors used an SLA (stereolithography) printer to create foams with a polymer resin pre-mixed with a blowing agent. This mixture was then expanded after post manufacturing, using heat. This work verifies and expands the existing results by studying the effect of distinct types of structural infill inside the part and investigating the morphology and behavior of the resulting foam structures.

## 1.1. Objectives

This research work aims to develop a process to produce polymeric foams through additive manufacturing.

The main aims of this research work are:

- To study a method to produce foams additively, bubble by bubble without foaming agents.
- To study a method to produce pre-forms using additive manufacturing and expand the resulting parts using a blowing agent activated by heat.
- To study the parameters of the above methods and overall feasibility.

## 1.2. Structure of the report

This report has been organized into four chapters.

- Chapter I contains the study's introduction and a description of the issue, as well as its main aims.
- Chapter II is the Literature Review. It focuses on Additive Manufacturing Technologies, VAT Photo-Polymerization, Polymerization Processes, and Materials.
- Chapter III Contains the description of the experimental work, which is divided into concepts 1 and 2, as well as chemicals, equipment, and experimental process.

- Chapter IV: Result and Discussion as this includes the findings of several specimen characteristics, includes expansion, shrinkage, mechanical testing, and micro-CT of specimens.

# 2. Literature Review

## 2.1. Additive Manufacturing technologies

According to Berman (2012), 3D printing is the computer-controlled sequential layering of materials to create three-dimensional shapes. It is also referred to as additive manufacturing (AM). It is particularly useful for prototyping and manufacturing of geometrically complex components.

AM is a rapidly growing field, having an impact in multiple industries, revolutionizing design, and simplifying the processes to go from a 3D model to a finished product. Comparing AM with other manufacturing processes such as molding processes, where the material is deposited in a mold that has the desired shape, and subtractive processes, where a solid piece of material is cut into the desired shape, molding processes require the production of the mold to manufacture a product in mass quantities, and subtractive processes produce waste material, as the material being cut is not reused. AM can advantageously create a wide range of shapes without the need for mold and only using the required material (Kruth, Leu, and Nakagawa 1998).

This following are applications in which AM is frequently used are (Ma and Wang 2018; Kafara et al. 2017):

- The fabrication of customized freedom building components.
- The decrease of material usage and environmental impact.
- The fabrication of functionally graded components.

Additive Manufacturing can process a variety of materials. with little material waste, less labor intervention, and quick manufacturing. According to the ASTM/ISO (ASTM 2010), Additive Manufacturing processes are classified as:

- VAT Photopolymerization.
- Sheet lamination.
- Binder jetting.
- Material extrusion.
- Powder bed fusion.
- Direct energy deposition
- Material jetting.

Additive manufacturing is being investigated in several fields such as the fashion industry (Sun and Zhao 2017), prosthodontics (Torabi et al. 2015), industrial applications for aerospace and automotive manufacturing (Lim et al. 2016), medical applications (Yan et al. 2018) (Melchels et al. 2010), prototyping models for aesthetic and functional testing (Galati and Minetola 2020) and in solutions for the construction industry (Craveiro et al. 2019).

The concept of 3D printing was developed in the late 1980s. Since then, several technologies of additive processes were developed that have the potential to revolutionize manufacturing. (Mohamed et.al 2015). At this stage, rapid prototyping (RP) technologies were used to produce prototypes for products used in the manufacturing sector. For instance, Arthur et al. (1996) used RP technology to develop electrodes for electrical discharge machining (EDM). Vinodh et al.

Additive Manufacturing (AM) has become an integral part of modern product development and continued to play a significant role in the manufacturing industry in the 21st century (Feixiang, Liyong, and Xia 2016). At the end of the 20 th century, technology has been commercialized to the extent where machines are now affordable for use at home (Bradshaw et al., 2010).

## 2.2. Vat Photo-polymerization

Vat photopolymerization is one of the most popular techniques of 3D printing. Photopolymerization technique is used by different 3D printing processes such as 3D Digital Light Processing (DLP), Stereolithography (SLA). SLA and DLP are two different approaches to Vat Polymerization technologies. Both start from a liquid to solidify the desired object by the action of light, which activates the polymerization reaction.

When it comes to building 3D objects, a vat polymerization process is a viable option because of its high resolution, wide range of input materials, and dimensional accuracy. Mechanical designs that restrict printing to a single photocurable resin during vat polymerization limit the capacity to spatially regulate the placement of several components, making it difficult to produce complex structures with integrated functionality.

Vat photopolymerization technology has recently become more widely available, however there are still substantial limitations in the market. Vat photopolymerization is inappropriate for many sophisticated quick prototyping applications due to resource limitations and multi-material printing, and among several additive manufacturing technologies, the family of vat photopolymerization is a group of technology that can maintain a higher accuracy in terms of shape accuracy and complexity. The principle of vat photopolymerization is used by stereolithography (SLA) and digital light processing (DLP) where the process starts from a liquid to solidify a desired object in the presence of light (Taormina et al. 2018).

Workflow for Vat Photopolymerization involves the following steps:

**Pre-processing:**

The initial step for the AM process is the development of a 3D model with the use of computer aided design (CAD) software or 3D scanner. The data is prepared with the help of standard triangulation language (STL), where the 3D model is converted into a STL format. (Pagac et al. 2021).

**Processing:**

The CAD design is sent to the printer must be fabricated in layers. These layers are supported by each other or by a platform or other support elements. The STL model after proper designing and orientation are divided into layers, known as slicing. The sliced layers are sent to the printer for printing (Pagac et al. 2021).

**Post Processing:**

During this process, the printed model is removed from the platform and refining is performed to obtain the finished product. During Photopolymerization, the final product is rinsed in a wash solution for example isopropyl alcohol (IPA) to remove the resin. The printed product must ensure the mechanical strength, thus, to enhance the mechanical properties, the built models are cured artificially with ultraviolet light or exposed to sunlight (Pagac et al. 2021).

## 2.3. Classification of Vat photopolymerization

Photopolymerization can be classified according to the method of curing. The Stereolithography (SLA) uses LASER, digital light processing (DLP) uses digital projection and continuous digital light processing (CDLP) uses light emitting diodes and oxygen (Pagac et al. 2021) Figure 2-1.

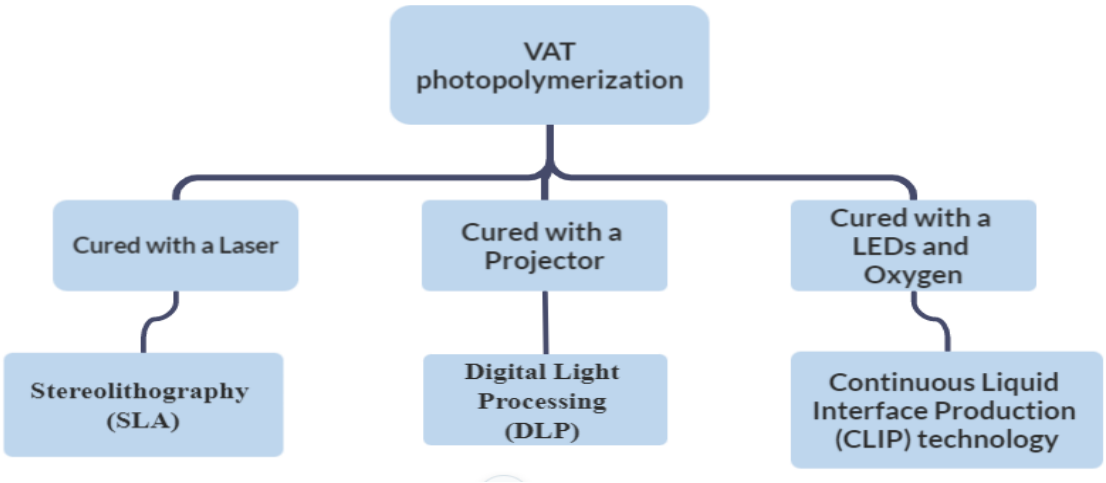


**Figure 2-1 Types of curing methods for Vat Photopolymerization (Pagac et al. 2021)**

### 2.3.1. Stereolithography (SLA)

Stereolithography is the first commercially available additive manufacturing technology. It is a solid freeform technique (SFF) that was introduced in the late 1980s (Melchels et. al, 2010). Although many other techniques have been developed since then, stereolithography remains one of the most powerful and versatile of all SFF techniques as it has the highest fabrication accuracy (Kruth et al. 1998)

The stereolithography apparatus consists of four main parts. It has a tank/vat that is filled with liquid photopolymer. It has a platform or elevator that can be lowered into the tank. Stereolithography uses a UV LASER for photopolymerization of the photosensitive polymer. A computer controls the platform and the laser. The computer also stores the file, CAD model that is to be printed. In the initial stage, a thin layer of laser or photopolymer is exposed on the platform. When the laser hits the platform printing the pattern of the object beam printer, the resin hardens instantly when it encounters the UV laser forming the first layer of the object. Due to the absorption and scattering of the beam, this reaction only takes place near the surface. This produces parabolic cylindrical voxels (three-dimensional pixels which are characterized by their horizontal line width and vertical cure depth (Pham and Gault 1998).

The computer will direct the laser according to the geometry of the CAD file. Once the initial layer has hardened, the platform is lowered. The recoated blade moves across the platform to apply the next layer of resin. The laser again traces the next cross-section of the object which instantly burns to the previous layer. This process is repeated until the entire object is formed.

Once the object is completely printed, it is removed from the tank and dipped into the liquid solvent bath. This gets rid of excess photopolymer on the object. The supports that are used in the creation of objects are clipped off. The object is baked in an ultraviolet oven to further cure the object. Once the curing is over the object is ready for use. SLA prints high-quality parts at a fine resolution as low as 10μm (Wang et al. 2017)

Stereolithography is innovative as it can produce extremely complex geometry with ease which is not possible with traditional manufacturing. The technique can produce smooth and high-quality surfaces and reduces non-productive recoat time (Pham and Gault 1998).

### 2.3.2. Digital Light Processing (DLP):

DLP uses a projector to cure photopolymer resin. This method is similar to the SLA method except that instead of using a UV laser to cure the photopolymer resin, light bulbs used, like the one used for office presentations or in-home theatre, to project the image of the cross-section of an object into photosensitive resin (Quan et al. 2020) Figure 2-2.

In the DLP technique, the object is either pulled out of the resin, which creates space for the uncured resin at the bottom of the container hence forming the next layer of the object, or down into the tank with the next layer being cured at the top. Free radical photosensitive resin is used for DLP 3D printing. The technology prints the object with high precision, so it can only print the model with small size and is mostly used in the fields of jewellery casting and dentistry for manufacturing dental crowns (Quan et al. 2020).

Lovo et al. (2020) used DLP to characterize the commercially available Vat photopolymerization resins.

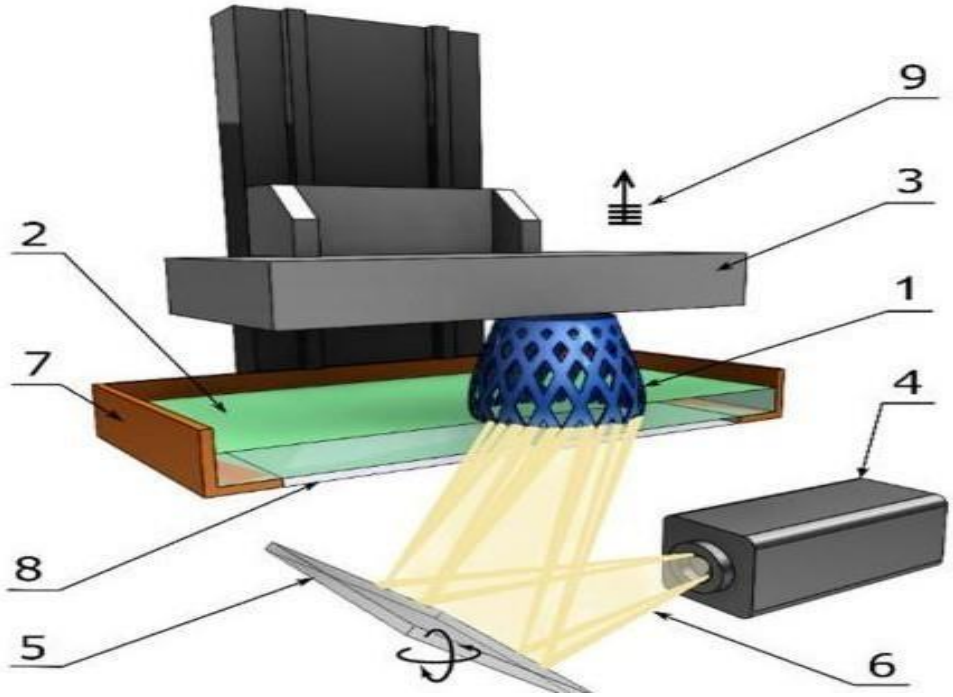


**Figure 2-2 Components of a typical DLP machine (Pagac et al. 2021).**

1. Printed part
2. Liquid resin
3. Building platform
4. Light source
5. Digital projector
6. Light beam
7. Resin tank
8. Window
9. Layer elevation

### 2.3.3. Continuous Liquid Interface Production (CLIP) technology:

CLIP technology is an advanced form of DLP which works by projecting a continuous sequence of UV images, generated by a digital light projector, through an oxygen-permeable, UV-transparent window below a liquid resin bath (Quan et al. 2020). The UV projection at the bottom of the tank maintains a stable liquid area due to oxygen inhibition. The special window provided at the bottom allows the light and oxygen to pass through. The dead zone created above the window maintains a liquid interface below the part. Above the dead zone, the curing part is drawn out of the resin bath (Balli et al. 2017)

## 2.4. Photopolymerization Process

Dr. Hideo Kodama is considered as the inventor of photopolymer technology. Kodama was a researcher in Nayoya Municipal Industrial Research Institute, who described the curing of a spatial model of photopolymer by exposing to ultraviolet light (Pagac et al. 2021). Photopolymer based 3D printing is one of the important branches of additive manufacturing. Photopolymers can change their properties when exposed to ultraviolet light. Thus, these polymers are sensitive to light and can change their state from liquid phase to solid phase. The area exposed to ultraviolet light hardens while the unexposed region remains in liquid phase.

Generally, photopolymers exist in liquid phase. However, they can be stored in the form of sheets. Photopolymers can change their properties when exposed to light, but there are other polymers which can change their properties under exposure to heat or microwave. The easily available photopolymers are polyvinyl cinnamate, epoxies, acrylics, polyisoprene, polyimides etc. The photopolymers are used in stereolithography, while other technologies used various materials such as rubber, plastics, glass, papers, titanium, metals etc.

## 2.5. Photopolymers

Photopolymers exists in liquid as well as in the form of sheet. The most used photopolymer is ester of cinnamic acid which is produced by the reaction of cinnamic acid and alcohol in the presence of light (Printwiki 2021). The major elements that build photopolymers are binders, monomers, photo initiators and inorganic additives (Lovo et al. 2020). The inorganic additives may be added to photopolymers to enhance the properties of photopolymers such as chemical agents and colorants (Castle Island 2009).

### 2.5.1. Oligomers (Binders) and monomers

The basic building blocks for vat photopolymerization and are the major determinant of the properties of the photopolymer. A properly formulated binder inhibits undesirable self-heating, which causes material degradation, flaw, and distortion. (Mukhametov, Merkulova, and Chursova 2012). Thus, the properties of the binder influence the durability and heat properties of the material. Binders make up for more than half of the photopolymer's weight (Bagheri and Jin 2019).

Monomers or oligomers can be photopolymerized through radical or cationic mechanism in the presence of photo-initiators when exposed to visible lights and in ultraviolet light. They may result in premature polymerization, which can be stabilized using inhibitors. According to Mukhametov et al. (2012) during vat photopolymerization, the composition of binders should be such that it takes minimal time for curing. The authors produced an epoxide binder by resin transfer molding which were suitable for temperatures between –60 to +200 ºCand possess viscosity between 20 to 200 Pa/s. Mukhametov et al. (2012) described a thermo-reactive polymer binder with a predicted level of rheological and deformation properties for production of polymer composite materials by resin transfer molding.

### 2.5.2. Photo-initiators

The function of photo-initiators is to initiate the photochemical reaction. For the activation of photochemical reaction, photo-initiators of high molar extinction coefficients usually of short wavelength i.e., less than 400 nm are used. The wavelength of photon source can be 190 to 400 nm for UV, 400 to 700 nm for visible and 700 to 1000 nm for IR range (Bagheri and Jin 2019). The photo-initiator system should have high absorption coefficient for the conversion of photolytic energy into the reactive species (radical or cation). Such released reactive species acts as a catalyst among monomers and oligomers for chain growth through radical or cationic mechanism. The light irradiation can be through xenon lamps, mercury arc lamps, LEDs, or lasers (Bagheri and Jin 2019) Figure 2-3.

Schlögl et al. (2012) used 2,2-dimethoxy-2-phenylacetophenone as photo-initiator during the production of 3D structures in offset printing technique to find a balance between the speed of the ink and gas bubble foaming speed.

(Houbertz et al. 2004) studied the impact of photo initiators on the photopolymerization and determined the properties of inorganic-organic hybrid polymers. It was shown that the degree of polymerization increases with increasing Ultraviolet initiator concentration up to 3 wt %.

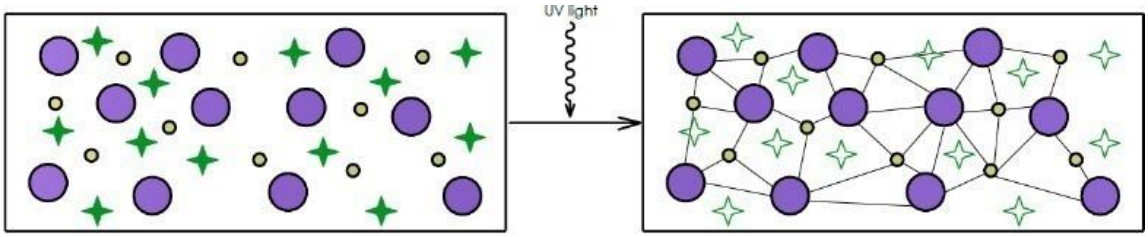


**Figure 2-3 Liquid photopolymer (on the left), stimulated polymerization by Ultraviolet (Pagac et al. 2021)**

### 2.5.3. Types of photo-polymerization

Photo-polymerization can take place through the following mechanisms:

- **Free radical photopolymerization:**

  Free radical photopolymerization is a process where light-sensitive photo initiator molecules such as (meth)acrylate present in liquid monomers react with photon particles of light to produce highly reactive free radicals. Initiation is the first step in the polymerization process. These free radicals developed are transferred to the double bond monomers to make them polymers to begin the polymerization process (Dendukuri et al. 2008). Most commonly, this technology uses multi and monofunctional monomers for building polymers with insoluble, infusible, and cross-linked characters.

- **Cationic photopolymerization:**

  The cationic polymerization reaction is a type of chain-growth polymerization in which a cationic initiator transfers charge from monomer to monomer during chain growth, which becomes reactive. This reactive monomer goes on to form a polymer. Lewis acids are the most common compounds used for the initiation of cationic polymerization. Cationic

polymerization reactions are sensitive to temperature. Both the reaction rate and molecular weight rapidly decrease with increasing temperature (Li et al. 2010).

- **Anionic photopolymerization:** The anionic polymerization reaction is a type of chain-growth polymerization where the polymerization of monomers is initiated with anions. This mechanism yields more regular polymers with less branching. There is not sufficient research related to anionic photopolymerization. Tsuchida et al. (1987) performed polymerization of epoxides by using catalyst titanium tetraisopropoxide and phenol or its derivatives for anionic photopolymerization of cyclohexene oxide.

## 2.6.Properties of photo-polymerized parts

Ahmad et al. (2020) studied the mechanical properties of photopolymer developed through stereolithography. They highlighted the importance of print orientation, resolution and Ultraviolet curing time and temperature on mechanical properties of printed parts. The mechanical properties were improved after Ultraviolet light curing at hot temperature.

The mechanical strength of a printed material is critical in addition to other properties. Lovo et al. (2020) studies of the mechanical strength of commercial photocurable resins are used for medical applications because they are biodegradable. Similarly, Medellin et al. (2019) discussed the importance of nanocomposites to enhance the material properties of vat photopolymerization resins. They explained that the application of nanocomposites provides reinforcement in terms of hardness, tensile strength, elongation, impact strength as well as the electrical conductivity of the final product.

## 2.7.Photopolymer Resins for SLA

**Standard resins:**

Accurate details and a smooth surface finish are provided by standard resins. The common resins offer precise features and a smooth surface finish and come in a wide range of colors, including white, black, translucent, turquoise, and blue. Rapid prototyping is made possible by the draft resin, which is included in standard resin and has a curing period that is 3–4 times faster than that of traditional standard resin. This resin's disadvantage is that the layer thickness fluctuates from 100 microns to 300 microns, giving the printed specimen's surface the appearance of a staircase (form labs 2021).

**Structural resin:**

Structural resins, like Grey Pro resin, can print objects with great precision, minimal elongation, and less creep. The high temperature resin in this family can endure pressures of 0.45 MPa and temperatures of up to 289 o C. (Pagac et al. 2021). Application: Molding templates, reusable functional prototypes, and conceptual modeling. This resin is most suited

for printing thin walls such as turbine blades, fans, electronic covers, etc. in the automobile industry.

**Tough and Durable resin:**

These resins are ideal for functional prototypes like jigs and clamps due to their great ductility, deformation, and impact resistance. Polyethylene or Polypropylene is used to make these resins (Pagac et al. 2021).

**Ceramic resin:**

The photopolymers contain silica within. Higher tensile strength is provided by this type of resin. The photopolymer network gets burned when the 3D printed items are baked in a kiln. The ceramic portion is what is left (Pagac et al. 2021).

**Castable wax resin:**

Castable wax resin creates pieces with precise finishing and detailing. Investment casting often uses this kind of resin. A wax fill is rendered inside of a ceramic mold and allowed to set. To create a part, wax is melted, and molten metal is put in (amfg 2018).

## 2.8.Production of foams

Foam is the type of material that can be used to produce more comfortable, safer, and lighter products. There are three types of foaming techniques: mechanical, chemical, and physical foaming.

**Physical foaming:**

Physical foaming involves mixing a polymer with a liquid at a low boiling point. Once low boiling point liquid has dissolved into the polymer and foamed, the mixture is heated and compressed Figure 2-4. The foams created using the physical foaming technique are lighter. With this approach, the desired part can be produced with less raw resources. Utilizing this technology, injection molding offers increased productivity (Jin et al. 2019).

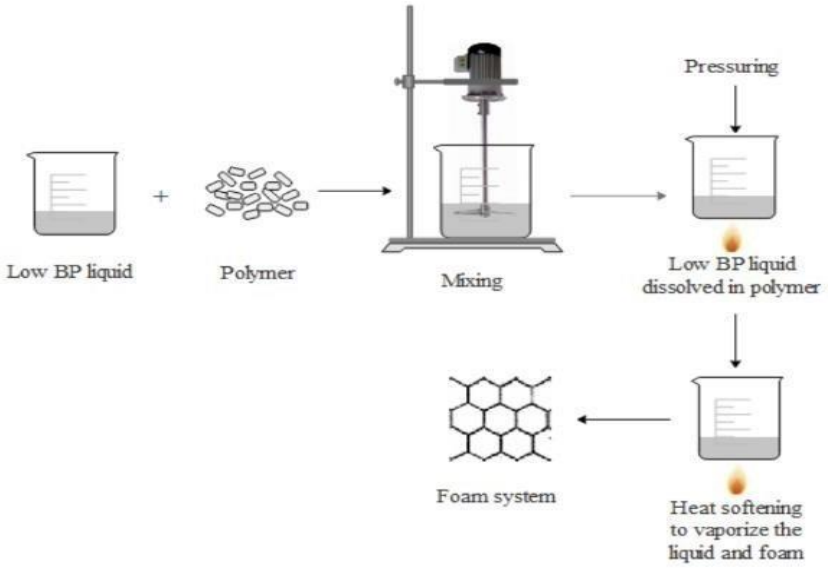


**Figure 2-4 Schematic diagram of physical foaming (Jin et al. 2019)**

## Mechanical Foaming:

The method of mechanical foaming involves adding air to the polymer resin. Mechanically stirring the resin causes it to froth Figure 2-5. As a result, this technique does not need a foaming agent.

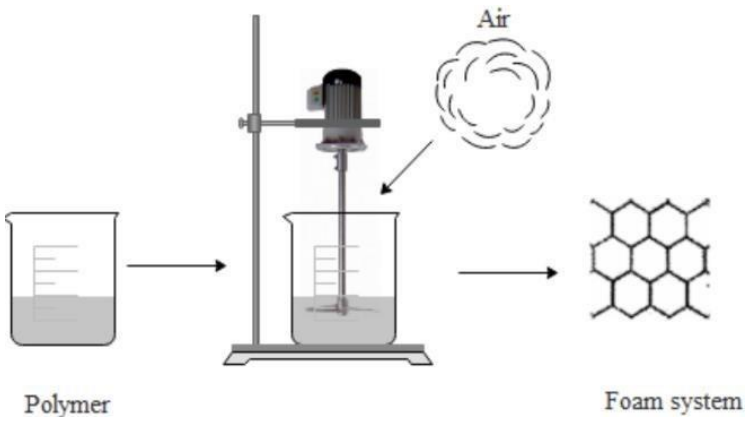


**Figure 2-5 Schematic diagram of mechanical foaming process (Jin et al. 2019)**

## Chemical Foaming:

There are two ways to implement chemical foaming: either by using a blowing agent or by having two polymers undergo a chemical reaction.

In the first case, the molten polymer is combined with a blowing agent Figure 2-6. The mixture is heated and compressed to create a foam system. In the second case, foamed

polymers are created by allowing the two polymers to combine chemically and form inert gases.

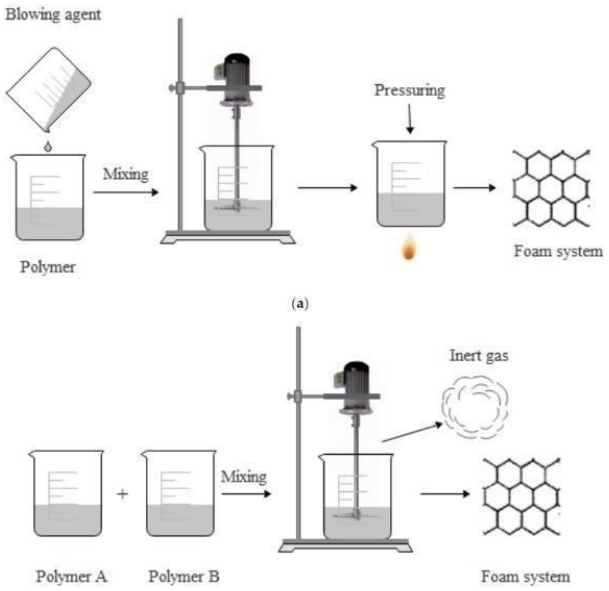


**Figure 2-6 Schematic diagram of chemical foaming (Jin et al. 2019)**

## 2.9. SLA printing of foam pre-forms

This study's goal is to create foams using physical and chemical blowing agents. Below are detailed explanations of the materials that can be used to produce foams or pre-foams by the SLA printer.

In 3D printed foams, the formulation of foaming resin presents a hurdle. For a suitable resin composition, blowing agent and monomers must work together in harmony. A highly expandable foaming prepolymer resin for lithographic 3D printing was investigated by Wirth et al. (2020) using the polymerization method. They created a foamy polymer resin that, when 3D printed, could swell up to 40 times its initial volume. According to the researchers, complicated shapes may be created using developed porous foam-based 3D printing, which has applications in biology, aerospace, architecture, and other fields. The researchers used a helical wind turbine that was 3D printed at one third scale and then expanded to the suggested size to demonstrate their claim.

The researchers employed a monomer called 2-hydroxyethyl methacrylate, an ideal photo initiator, and a blowing agent called di-tert-butyl decarbonate ($BOC_2O$) to pair with the monomer to create the right foaming material. For preventing precipitation during printing, the blowing agent must be soluble in monomer. The printed portions become unevenly expanded and inhomogeneous as a result of the precipitation. To prevent evaporation during printing, the blowing agent's decomposition temperature must be below melting or decomposition temperature and above the glass transition (Wirth et al. 2020).

The most used blowing agents in industry are as follows:

i) Di-tert-butyl decarbonate ($BOC_2O$)
ii) Aazodicarbonamide (ADC)
iii) p-toluene- sulfonhydrazide (TSH)
iv) sodium bicarbonate ($NaHCO_3$)
v) Water ($H_2O$), and
vi) Ethyl acetate (EA)

Therefore, the ideal blowing agent ought to be soluble in monomers and capable of producing a sizeable amount of gas. When activators like urea, citric acid, and zinc oxide are present, blowing agents like ADC and $NaHCO_3$ release a substantial volume of gas. The volatility of solvent-based blowing agents including toluene, ethyl acetate, and hexane is higher. Such blowing agents are undesirable for printing because they often evaporate from the resin bath. The following are the benefits and drawbacks of the blowing agent investigated by Wirth et al. (2020) while producing highly expandable foam for lithographic 3D printing:

**Table 1 The merits and demerits of blowing agent to produce expandable foams (Wirth et al. 2020)**

| Blowing agent | Thermolysis temperature | Advantages | Disadvantages |
|---|---|---|---|
| $BOC_2O$ | 196−220 | solubility, high gas production | toxicity |
| ADC | 150-190 | high gas production | insoluble in all monomers |
| TSH | 120-130 | Low decomposition temperature | Low gas production, poor solubility |
| $NaHCO_3$ | 160 | nontoxic, inexpensive, high gas production | insoluble, low gas |
| $H_2O$ | 100 | safe, miscible with | plasticizer for HEMA and |

Upon reviewing the paper by (Wirth et al. 2010), we came up with the following materials that we will be using to manufacture foams are listed below.

**Monomer:**

The most grilling part of the experiment was to determine the combination and the mixture aspects of the monomer and the blowing agent. To prevent evaporation during a multi-hour print, it was required to use a blowing agent with a decomposition temperature lower than that of HEMA (hydroxyethyl methacrylate) (Td = 230 °C), so HEMA (hydroxyethyl methacrylate) was selected for the monomer. (Wirth et al. 2020) because of its stability in

ambient circumstances, appropriate cure time, excellent mechanical characteristics, glass transition temperature above room temperature and high decomposition temperature.

**Optimization of Photo-initiator:**

After ensuring appropriate monomers, a more thorough screening process was conducted, which took photo-initiator species, concentration, and matching with an appropriate blowing agent into account. At 405 nm source of light, both diphenyl(2,4,6-trimethylbenzoyl) phosphine oxide (TPO) and phenylbis(2,4,6-trimethylbenzoyl) phosphine oxide (BAPO) generated a quick cure. For many of the studied monomers, including HEMA, BAPO/TPO in a 1:1 molar ratio was exceptionally adaptable and achieved the greatest cure performance. (Wirth et al. 2020)

**Blowing agent:**

$BOC_2O$ offers various benefits, including solubility, high gas production, and the ability to thermolyze at low temperatures. (Wirth et al. 2020) It has also been discovered that $BOC_2O$ is inert toward the HEMA monomer and that the solution is chemically stable when mixed for up to one week.

Experiments and the procedures are dicussed below for the expansion of the foams using the additive manufacturing of foamed structures.

# 3. Experimental work

In the following chapter, the materials, equipment's, and experimental procedure are discussed. The experiments were conducted to develop a process to produce bubble based polymeric material through additive manufacturing, cell by cell, to develop foams with or without foaming agents. Thus, the experiments were divided into two parts:

- Production of bubble in the Foam with Physical blowing agent (Concept 1)
- Production of bubble in the Foam with Chemical blowing agent (Concept 2).

## 3.1. Concept 1

This objective of this experiment is to the Production of bubbles in the resin using a physical blowing agent.

### 3.1.1. Materials

For the experiments, an ANYCUBIC 3D Printer Resin, 405nm SLA UV-Curing Resin was used Equipment

The list of equipment used for the experiments was.

- DLP projector (Acer)
- A syringe for pumping the air inside resin.

### 3.1.2. Experimental Procedure

To form the bubble inside the photo polymeric resins using DLP method, the first effort was made to inject air into the photo polymeric resin using a syringe Figure 3-1. By pumping the air inside the resin using the syringe thereafter exposing the resin with the digital light process. Two input parameters were selected, that is time and the height of the DLP machine above the resin. Then, efforts were made to form more bubbles inside the material by taking other parameters i.e., number of pumps (injecting the resin with the syringe and ejecting it), thus forming multiple amounts of air trapping inside the resin.

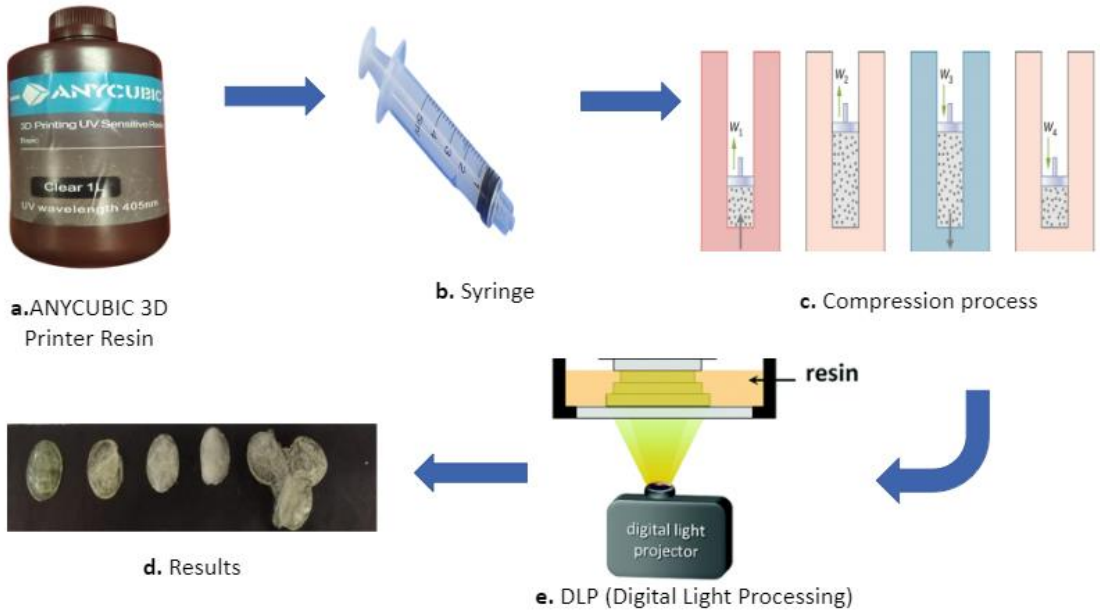


**Figure 3-1 Experimental procedure for concept 1 a) Resin for 3D printing b) syringe for pumping the air inside the resin c) process illustrates the compression process inside the syringe d) exposure of the resign above the DLP projector for curing e) cured parts**

## 3.2. Concept 2

The objective of this experiment is to produce a foam using a Chemical blowing agent.

### 3.2.1. Materials

The list of materials used for the experiments is shown below. As the materials below used on the base of Section 2.9 of the literature review.

- HEMA (hydroxyethyl methacrylate)
- (TPO) diphenyl(2,4,6-trimethylbenzoyl) phosphine oxide
- (BAPO) phenylbis(2,4,6-trimethylbenzoyl) phosphine oxide
- BOC2O (Di-tert-butyl decarbonate)

### 3.2.2. Equipment

The List of Equipment used for the experiments is listed below.

- Printing of part was conducted on SLA printer ANYCUBIC PHOTON.
- CAD and slicing of part were conducted using Lychee Slicer 3.
- Vacuum chemical chamber used because of toxicity of BOC2O.
- Industrial furnace used for expansion of foams.
- For measuring the parts vernier caliper was used.
- Skyscan 1174, Bruker used for CT scan of the samples

### 3.2.3. Experimental Procedure

There are several steps involved in the preparation of these tests.

- Modelling and slicing of the part to prepare it for SLA printing.
- Preparation of the chemical mixture for SLA printer to print the Part.
- Determining the parameters of the SLA printer and printing part.
- Post-processing of the part for the expansion.

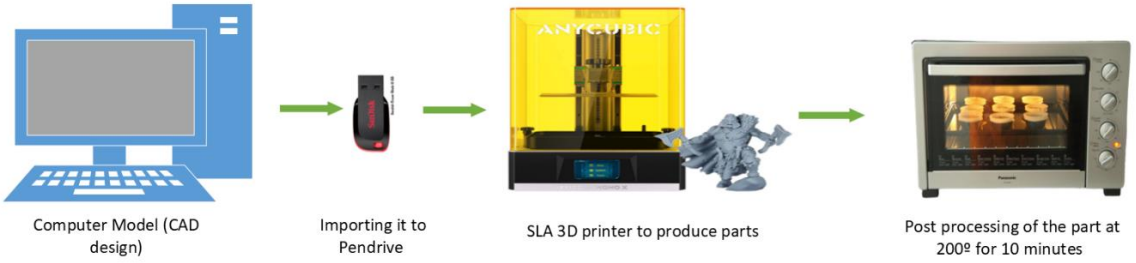


**Figure 3-2 Experimental Procedure Concept 2**

## Modelling and slicing of the part to prepare it for SLA printing.

Lychee Slicer 3 and Solid works were used to create the parts in the figure below because the initial goal of this experiment was to model the part with the infill structure inside so we could conduct additional research on the infill. This is because in the research of Wirth et al.

(2020) there was no infill introduced in the parts. So, to examine the effect the infill to the foams, cubes of 10 mm height and 10 mm radius were modelled and three infill structures - 100%, 75%, and 50% were used - Table 2.

**Table 2 Types of Infill structures**

| **a**: 100% | **b**: 75% | **c**: 50% |
|---|---|---|
|  | 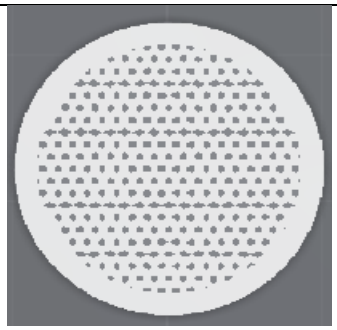 | 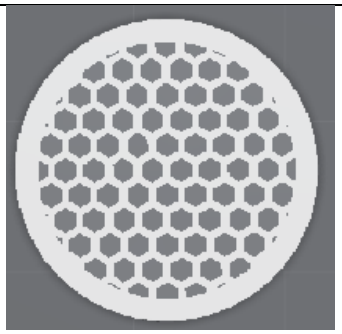 |

## Preparation of the chemical mixture for SLA printer to print the Part.

We used exhaustion chemical chamber for preparing three mixtures of samples with various amounts of monomer: 2- hydroxyethyl methacrylate (HEMA), photo-initiator: Phenylbis(2,4,6-trimethylbenzoyl) phosphine oxide (BAPO) and Diphenyl(2,4,6-trimethylbenzoyl) phosphine oxide (TPO), and blowing agent: di-tert-butyl dicarbonate (BOC2O) for the tests in order to create the chemical composition to form the resin used for the SLA printing, we were inspired by a research study by (Wirth et al. 2020) to create the mixing formula. Given that the SLA ANYCUBIC PHOTON printer can accommodate up to 125 ml of resin, we chose to produce 100 ml of each resin for printing, as shown in the table Table 3.

**Table 3 Chemical mixture with the expansion ratio observed by Wirth et al. (2020)**

| Sample | Monomer | Wt. % | Photo initiator | Wt. % | Blowing agent | Wt. % | Expansion ratio |
|---|---|---|---|---|---|---|---|
| A | HEMA | 93 | BAPO/TPO 1:1 | 5 | BOC2O | 2 | 50% |
| B | HEMA | 90 | BAPO/TPO 1:1 | 5 | BOC2O | 5 | 250% |
| C | HEMA | 85 | BAPO/TPO 1:1 | 5 | BOC2O | 10 | 750% |

# Determining the parameters of the SLA printer and printing part.

The SLA printer's default parameters prevented the sample from adhering to the built platform as shown in Figure 3-3.

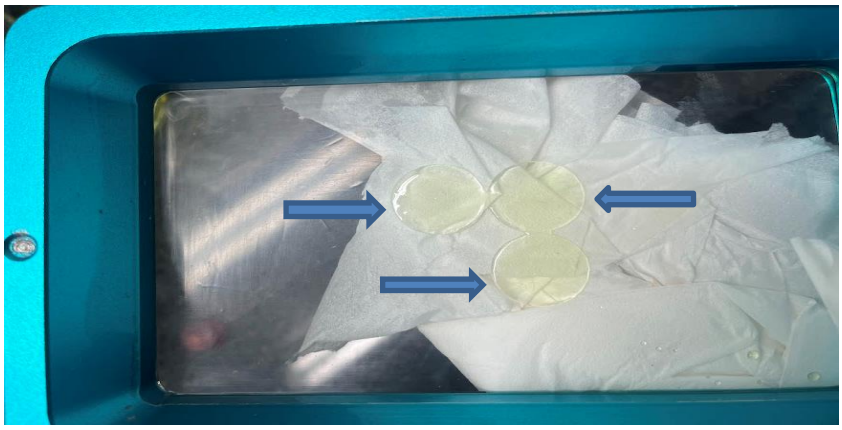

**Figure 3-3 Defected specimen before determining parameters**

Thus, it was crucial to adjust the parameters to get satisfactory results when the initial sample and started to print for this reason and researched the printer parameters from the work of (Wirth et al. 2020) and to find the optimal settings that will enable to print the part precisely. The parameters are to activate the blowing agent contained in the sample, are shown in Table 4. Following this tuning of the parameters, the printed part turned out well as in Figure 3-4.

**Table 4 SLA Printer Parameters**

| Burn In Layers | | Normal Layers | |
|---|---|---|---|
| Number of layers | 6 | Layer Thickness | 50 um |
| Exposure Time | 60 seconds | Exposure Time | 40 seconds |
| Light-off Delay | 3 seconds | | |

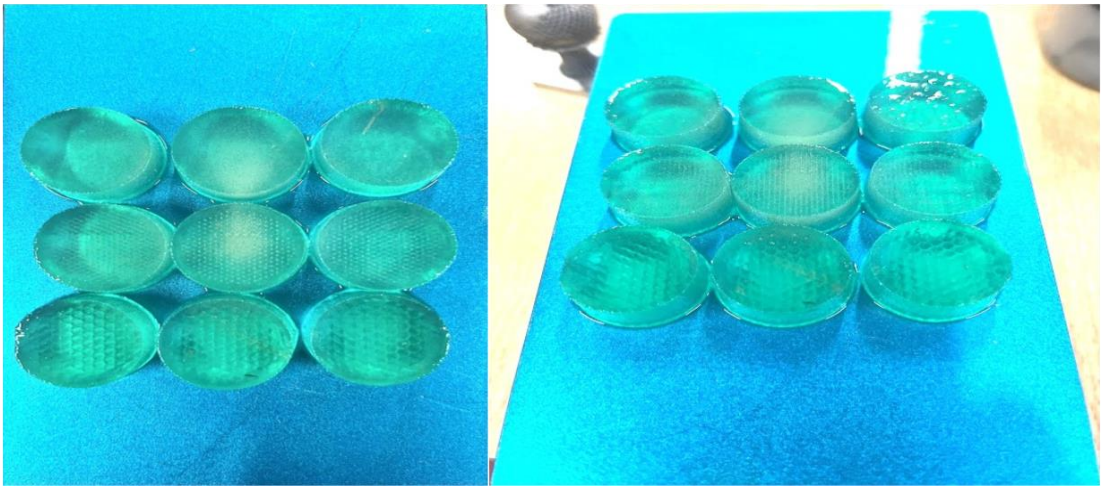

**Figure 3-4 Printed Parts from SLA printer**

## Post-processing of the part for the expansion.

Then after the part was produced in the SLA printer, the next post-processing step was to perform the thermal expansion. To do this, we placed a sample inside a furnace set to 200 degrees for 10 minutes to obtain the desired results as shown in the Figure 3-5

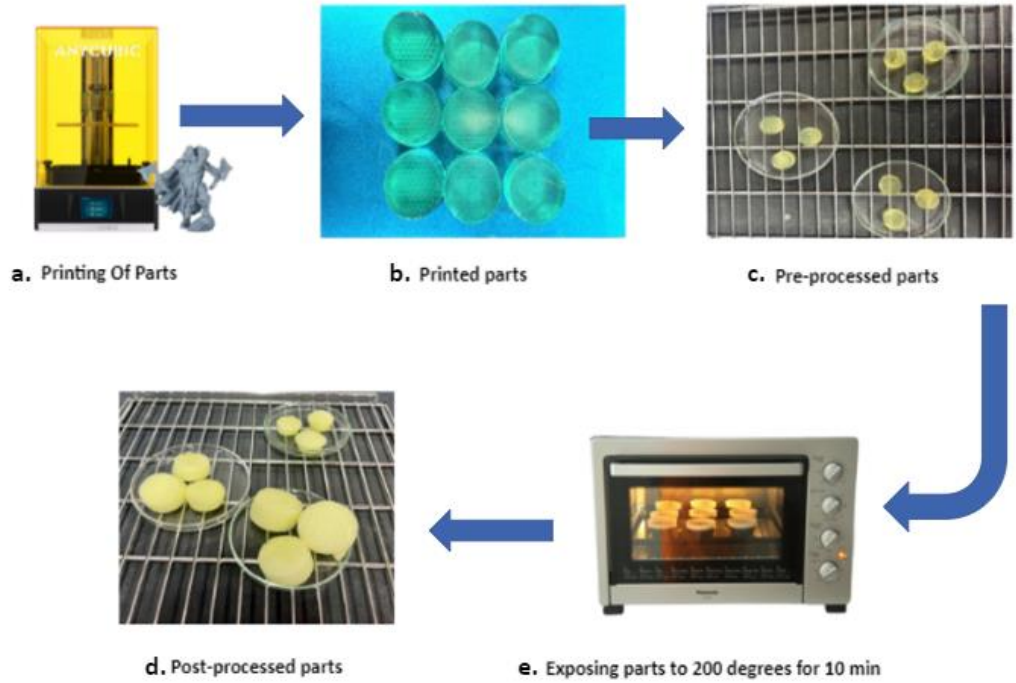


**Figure 3-5 Specimen Expansion Procedure a) printing of the samples using the SLP processes b) cured parts after SLP printing c) pre-processed parts , distributed the parts according to their infill d) processing the parts using**

**the furnace at 200 degrees for 10 minutes e) post-processed parts as we can see the significant amount of the expansion**

### 3.2.4. Evaluation

To evaluate the post-processed foams, the sample printed three times of each infill in two sets, one week apart as shown in the Figure 3-6.

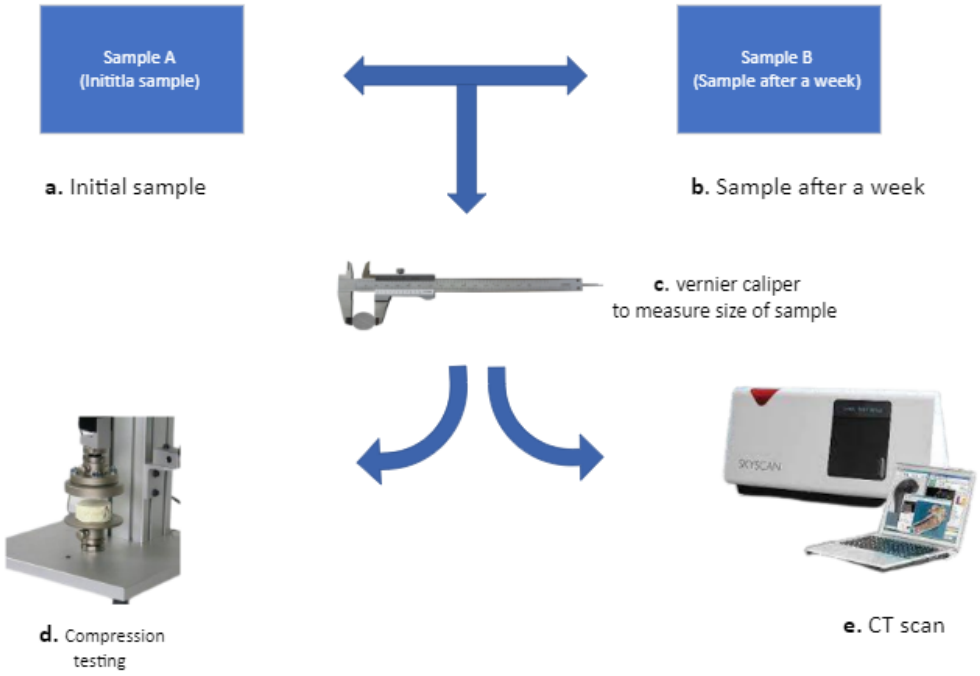


**Figure 3-6 Evaluation process for the parts a) sample A -initial sample b) sample B- sample taken a week apart c) measuring both the parts in order to get the difference i.e., from initial sample and sample taken week apart d) Mechanical compression testing of the parts e) CT scanning the parts in order to determent the porosity.**

And observed that once expanded, a part shrinks in size over time, so we measured the parts two hours apart after the initial printing of the post-processed foams. Compression testing was conducted to characterize the samples and CT scan was conducted to determine internal parameters of the structure.

# 4. Results and Discussion

## 4.1. Concept 1

We found the variations based on number of pumpings injected inside the photo polymeric resins, as per experimental work. The amount of air trapped inside the material is directly correlated to pumpings of the air. Transparency decreases of material after injecting maximum number of pumping in photo polymeric resins because many air bubbles formed. As shown in the Figure 4-1.

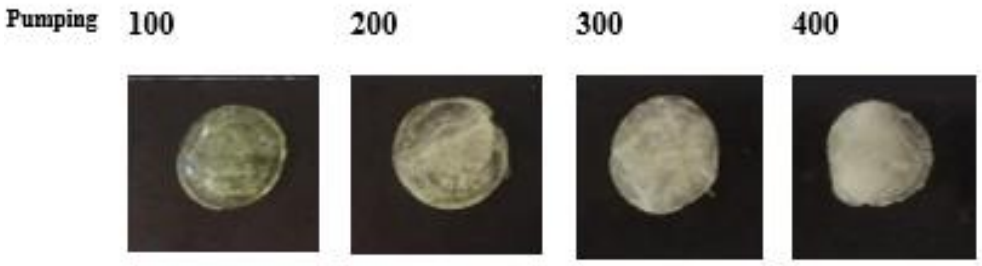


**Figure 4-1 Pumping vs Bubbles in specimen**

**Table 5 Time VS height of exposure**

| Time | Height |
|---|---|
| 10.9 | 100 |
| 8.24 | 85 |
| 8.46 | 75 |
| 7.86 | 65 |
| 7.15 | 42.2 |
| 6.74 | 40 |
| 5.80 | 38.3 |
| 4.36 | 36.2 |

Curing time and the height of the exposed light is directly proportional to each other, as we can see in the table decrease in the height of exposed light, time also decreases.

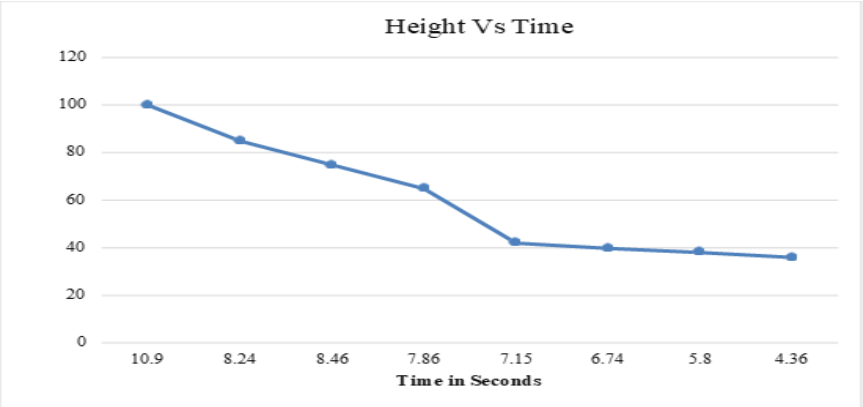


**Figure 4-2 Height Vs time Graph**

The physical method's results for Concept 1 were inapplicable because they did not demonstrate any expansion.

## 4.2. Concept 2

### 4.2.1. Expansion

A blowing agent was used for the experiments, as described in section 2.8. The foams that expanded the most have been seen in the **Figure 4-3**. As sample B received the most total expansion, while sample C received least amount of expansion, while sample A an experienced 273.89% of expansion. However, sample C was supposed to exhibit the greatest degree of growth by the research paper (Wirth et al. 2020), but it did not, therefore sample A and B were further analysed and for Sample C it needs further investigation.

In the figure43, the samples A and B exhibit the same pattern of expansion regarding the amounts of the monomer (HEMA) and the blowing agent (BOC2O) used in the mixture, with the blowing agent used in sample B having a weight of wt. of 5% ,Sample A having wt. of 2% whereas for sample C we used 10%, and the monomer used in sample B having wt. of 90%, Sample A 95% wt and for Sample C 85% wt respectively, as shown in table2 .

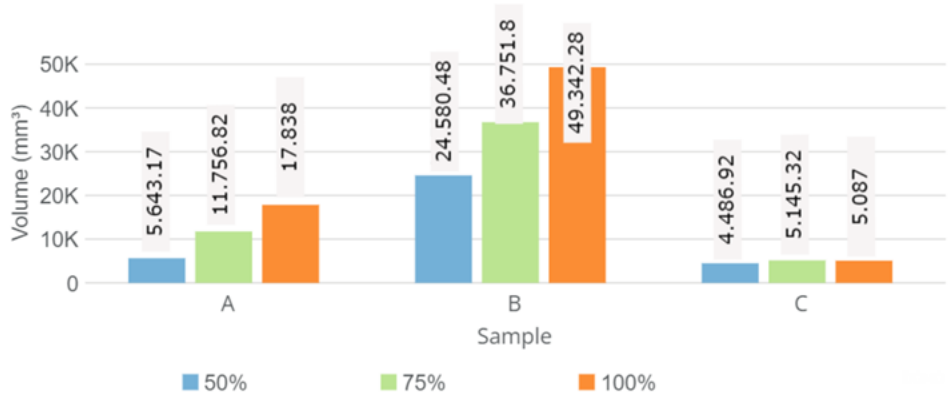


**Figure 4-3 Expansion of the Samples**

However, in this experiment, the observed expansion of specimens was significantly greater than that of the research paper. This difference in the expansion has been noted in Table5 and requires further research to validate the difference.

**Table 6 Difference in exansion of sample**

| Sample | Initial volume | Avg volume | Avg expansion | Expansion observed in literature | Difference in expansion |
|---|---|---|---|---|---|
| A | 3141.6 | 11746.00 | 273.89% | 50% | 223.89% |
| B | 3141.6 | 36891.52 | 1074.29% | 250% | 824.29% |
| C | 3141.6 | 4906.41 | 56.18% | 750% | -693.82% |

### 4.2.2. Effect of Infill

The quantity of infill in the sample's foams also plays a considerable influence. As seen in the accompanying figure, the sample with 100% infill saw the greatest amount of expansion, followed by samples with 75% of infill and 50% of infill, which experienced the least amount of expansion.

The correlation table above in the figure exhibit sample B with all three types of infill (100 %, 75 %, and 50 %, respectively) has experienced the greatest amount of expansion, whereas the sample A has experienced the least amount of expansion.

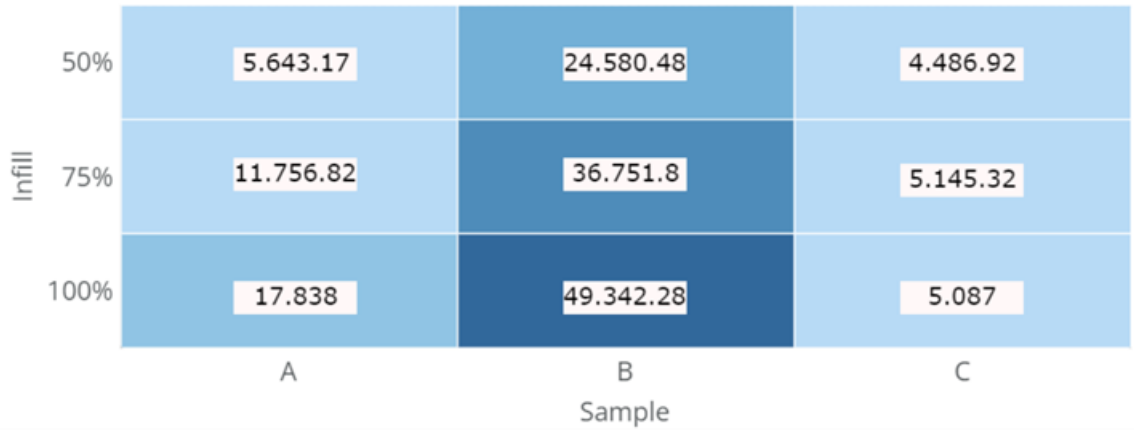


**Figure 4-4 Heatmap of Volume of specimen by sample and infill**

**Table 7Average expansion ratio**

| Sample | Infill | Initial volume | Avg volume | % Expansion | Avg % expansion |
|---|---|---|---|---|---|
| A | 50% | 3141.6 | 5.643.17 | 79.63% | 273.89% |
| A | 75% | 3141.6 | 11.756.82 | 274.23% | |
| A | 100% | 3141.6 | 17.838.00 | 467.80% | |
| B | 50% | 3141.6 | 24.580.48 | 682.42% | 1074.29% |
| B | 75% | 3141.6 | 36.751.80 | 1069.84% | |
| B | 100% | 3141.6 | 49.342.28 | 1470.61% | |
| C | 50% | 3141.6 | 4.486.92 | 42.82% | 56.18% |
| C | 75% | 3141.6 | 5.145.32 | 63.78% | |
| C | 100% | 3141.6 | 5.087.00 | 61.92% | |

### 4.2.3. Shrinkage along time

Samples responded differently when we measured the volume of a sample after first printing, after initial printing for two hours Figure 4-5, and after one week Figure 4-6.

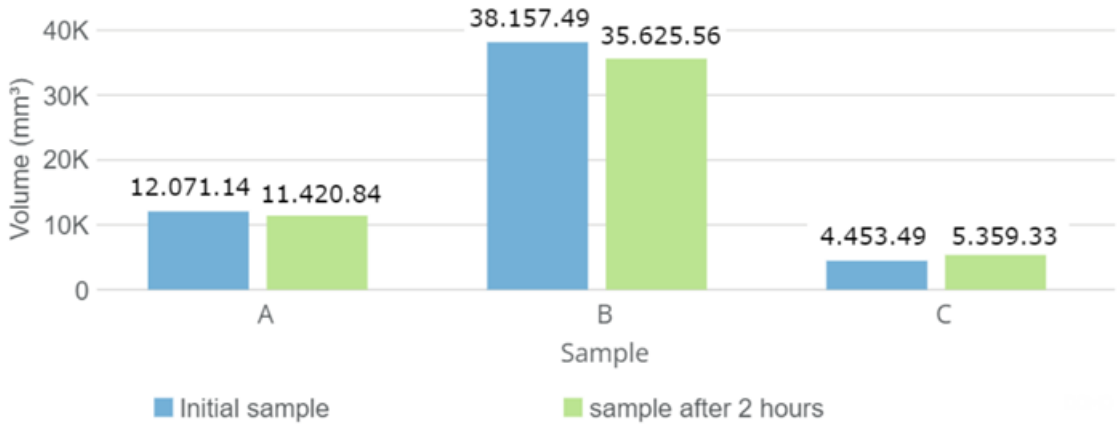


**Figure 4-5 Shrinkage in specimens after 2 hours**

When measured a week apart, samples A and B exhibited a reduction in average volume, but sample C increased considerably when measured for the second time.

**Table 8 Shrinkage in specimen after 2 hours**

| sample | Initial sample | After 2 hr | % Shrinkage | Avg Shrinkage |
|---|---|---|---|---|
| A | 12071.14 | 11420.84 | 5.693976975 | 4.99% |
| B | 38157.49 | 35625.56 | 7.107060212 | |
| C | 4453.49 | 5359.33 | 2.159964949 | |

The average volume of the entire sample had dropped by 4.99 percent as seen in table when the foam was measured two hours after the initial printing, and by 9.95 percent by the time, it was evaluated a week later as seen in Figure 4-5and Figure 4-6 and Table 7 and Table 8.

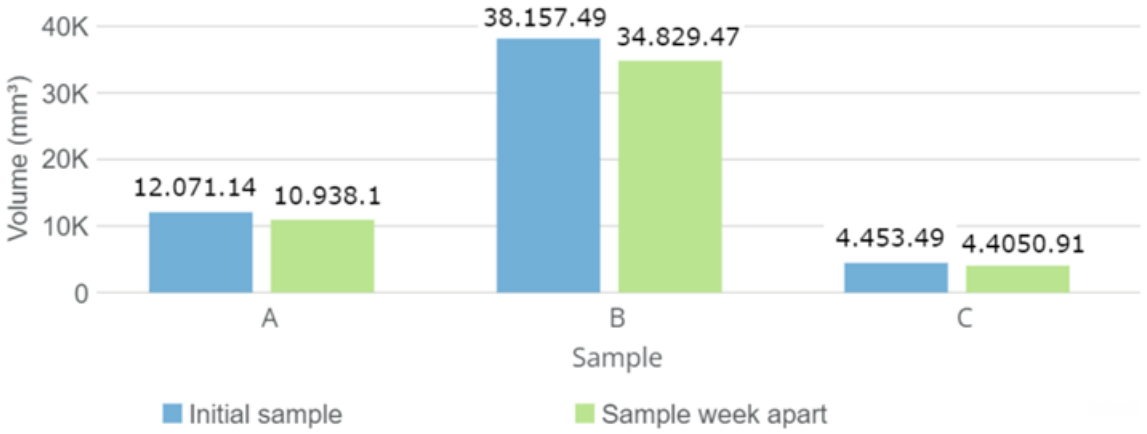


**Figure 4-6 Shrinkage in specimen week apart**

**Table 9 Shrinkage in specimen week apart**

| sample | Initial sample | week apart | % Shrinkage | Avg Shrinkage |
|---|---|---|---|---|
| A | 12071.14 | 10938.1 | 10.35865461 | 9.95% |
| B | 38157.49 | 34829.47 | 9.555184159 | |
| C | 4453.49 | 4050.91 | 9.938013928 | |

### 4.2.4. Mechanical Testing of Foams.

A ZWICK Z100 tensile test machine, in which the material is inserted, is utilized for the mechanical testing. A load is a force that is plotted against the displacement, or change in length, of the material. The displacement is transformed into a strain value, and the load is transformed into a stress value. The size of each sample used for the Mechanical testing are shown in Table 10.

**Table 10 Sample size description for Mechanical Testing**

| Sample | Infill % | Height (mm) | Diameter )mm) |
|---|---|---|---|
| A_50_1 | 50% | 13.86 | 30.04 |
| A_50_2 | 50% | 13.15 | 27.71 |
| A_75_1 | 75% | 16.01 | 32.77 |
| A_75_2 | 75% | 15.29 | 28.92 |
| A_100_1 | 100% | 19.25 | 34.19 |
| A_100_2 | 100% | 18.71 | 32.07 |
| B_50_1 | 50% | 16.67 | 38.88 |
| B_50_2 | 50% | 25.64 | 34.65 |
| B_75_1 | 75% | 25.19 | 43.17 |
| B_75_2 | 75% | 23.85 | 40.71 |
| B_100_1 | 100% | 31.91 | 45.82 |
| B_100_2 | 100% | 30.48 | 47.94 |
| C_50_1 | 50% | 11.38 | 21.57 |
| C_50_2 | 50% | 11.4 | 23.05 |
| C_75_1 | 75% | 11.79 | 24.13 |
| C_75_2 | 75% | 11.66 | 24.09 |
| C_100_1 | 100% | 12.08 | 22.86 |
| C_100_2 | 100% | 13.24 | 24.19 |

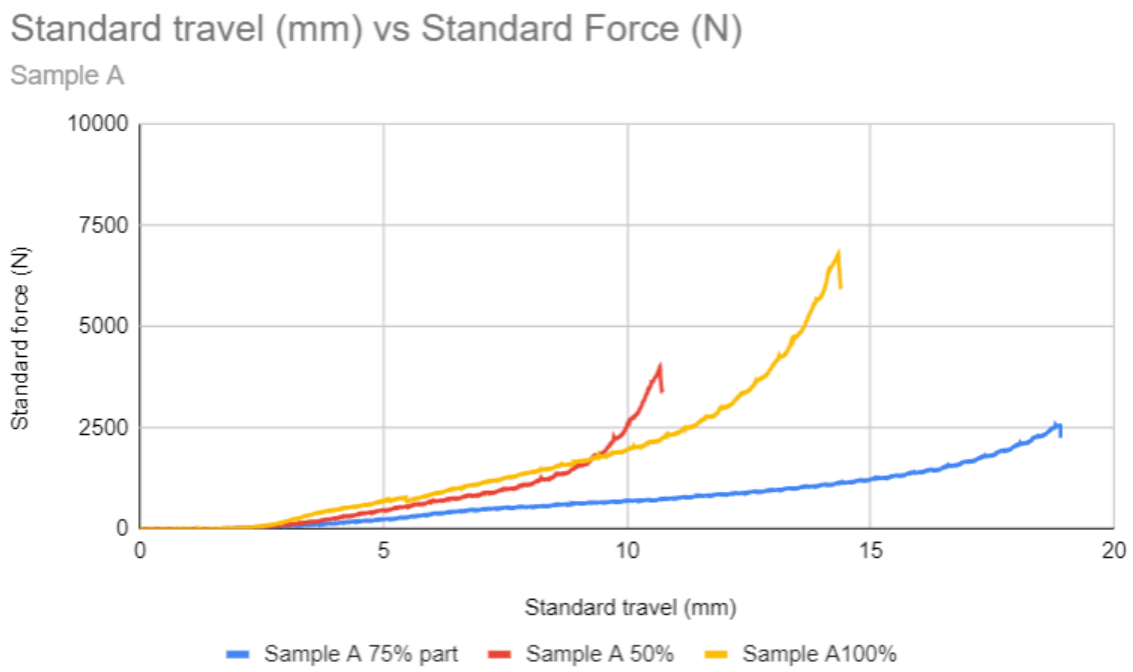


**Figure 4-7 Results of sample A including all infill**

As shown in figure 47, all the specimens from Sample A underwent the compression test with all three types of infill Structure, and as a result, we can observe that the specimen with 50% of infill was able to withstand less stress than the other specimens since the specimen's cell structure had not expanded as much as the rest of the specimens, and consequently, that specimens with 100% infill can withstand greater stress, followed by specimens with 75% because they had more material in the same volume.

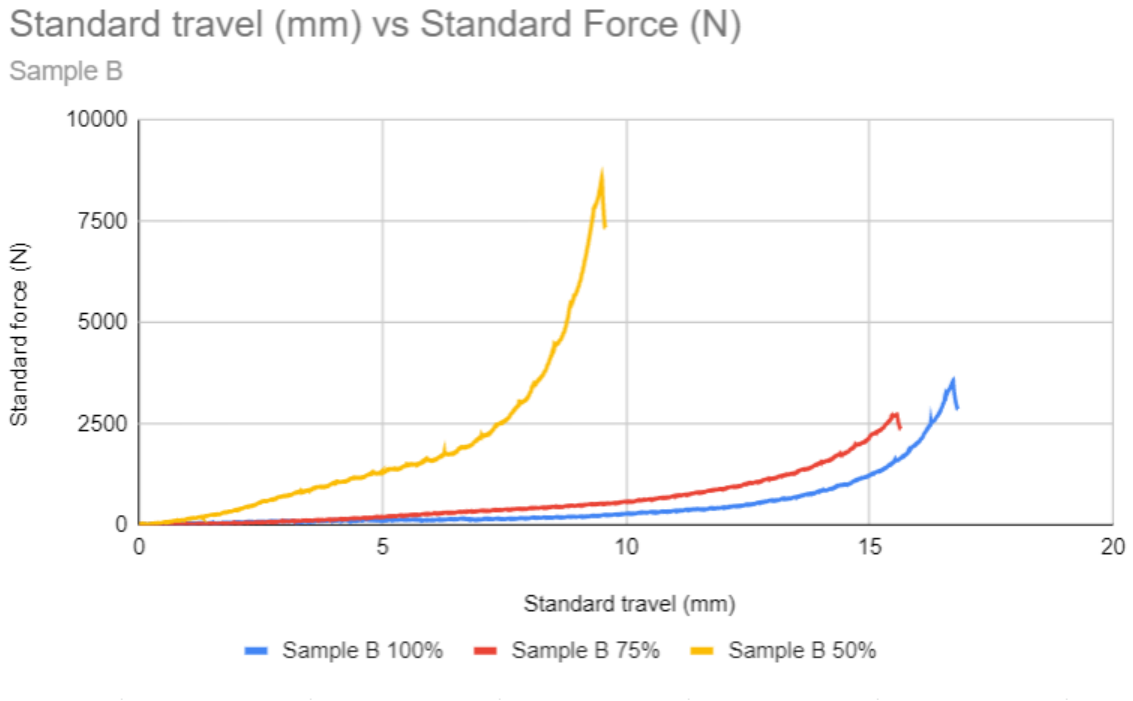


**Figure 4-8 Results of sample B including all infill**

In the figure 48, all the specimens with sample B were put through a compression test, and it is apparent that the specimen with 50% of the infill can withstand the maximum level of stress, while the specimens with 75% and 100% infill appear to follow a similar pattern or trend.

It is because sample B has the highest levels of expansion in the specimens at 75% and 100%, respectively, as seen in **Figure 4-3**, which caused their cell structure to become constrained and unable to withstand additional load, and for sample B which has 50% infill had modest expansion and consequently less void in its cell structure, it was able to withstand more load during the compression test.

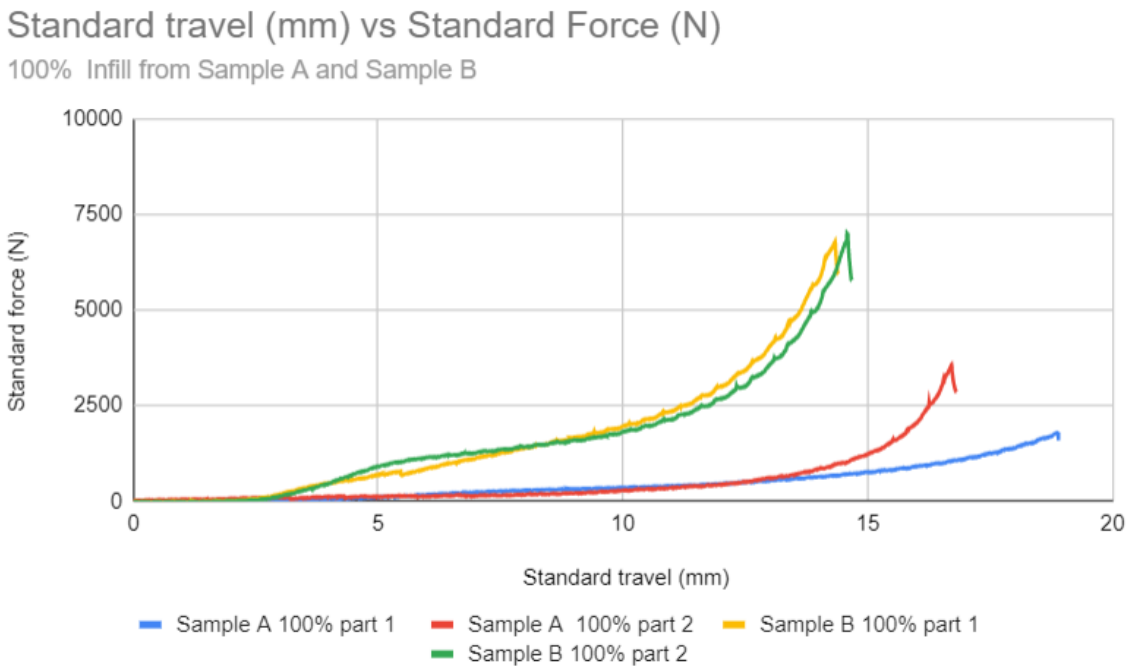


**Figure 4-9 Results of 100% infill of sample A and B**

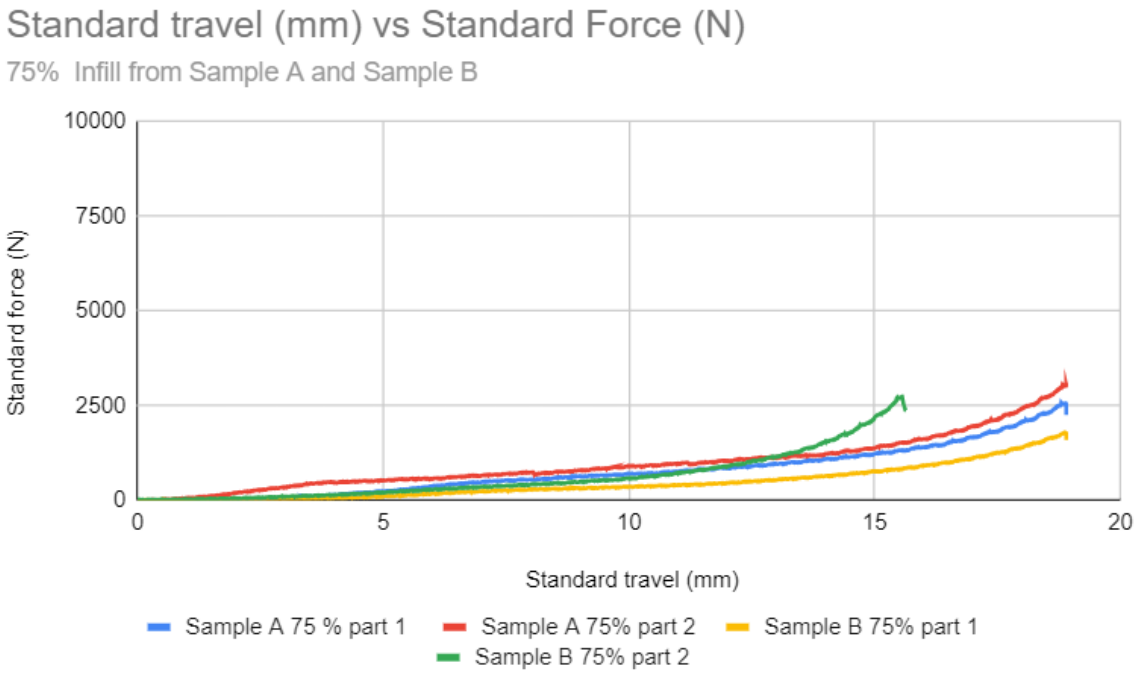


**Figure 4-10 Results of 75% infill of sample A and B**

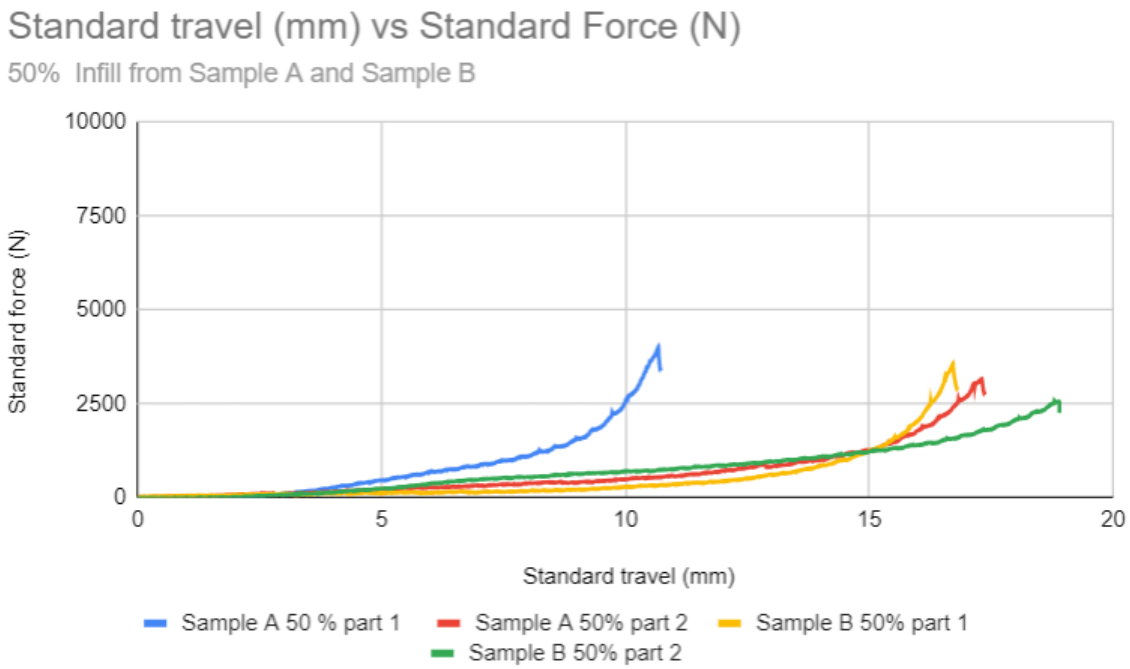


**Figure 4-11 Results of 50% infill of sample A and B**

To analyze the trend and pattern, we have classified the samples and their findings by their infill ratio Figure 4-9, Figure 4-10 and Figure 4-11, and we noticed that structures with more voids or spaces in their cell structures after expansion tend to have less strength, whereas those with less voids in their cell structures may sustain greater amounts of load.

### 4.2.5. CT Scan Results

The aim of the Micro-CT scan was to determine the characteristics of the cellular structure such as porosity. Equipment used to perform the scan was a Bruker Skyscan 1174.

The table includes the scanning parameters and the software used for scanning.

**Table 11 Scan Parameters and software used for CT scan**

| Scan parameters | Software used |
|---|---|
| Source Voltage (kV)= 50 | Skyscan 1174 |
| Source Current (µA)= 800 | NRecon version 1.7.0.4 |
| Image Pixel Size (µm)=22.70 | DataViewer version 1.5.2.4 |
| Image Pixel Size (µm)=22.70 | CTAn version 1.20 |
| Exposure (ms)=5500 | CTVox version 3.2 |
| Rotation Step (deg)=1.000 | |

**Table 12 CT Scan Results**

| Sample: B | Nº layers | threshold | ROI vol$^{m}$ | Object vol$^{m}$ | Porosity (total) |
|---|---|---|---|---|---|
| 100% | 255 | 37-255 | 5.70x1011 µm 3 | 1.28x1011 µm 3 | 77.60% |
| 75% | 255 | 43-255 | 5.70x1011 µm 3 | 1.26x1011 µm 3 | 77.90% |
| 50% | 255 | 53-255 | 5.70x1011 µm 3 | 1.77x1011 µm 3 | 69.00% |

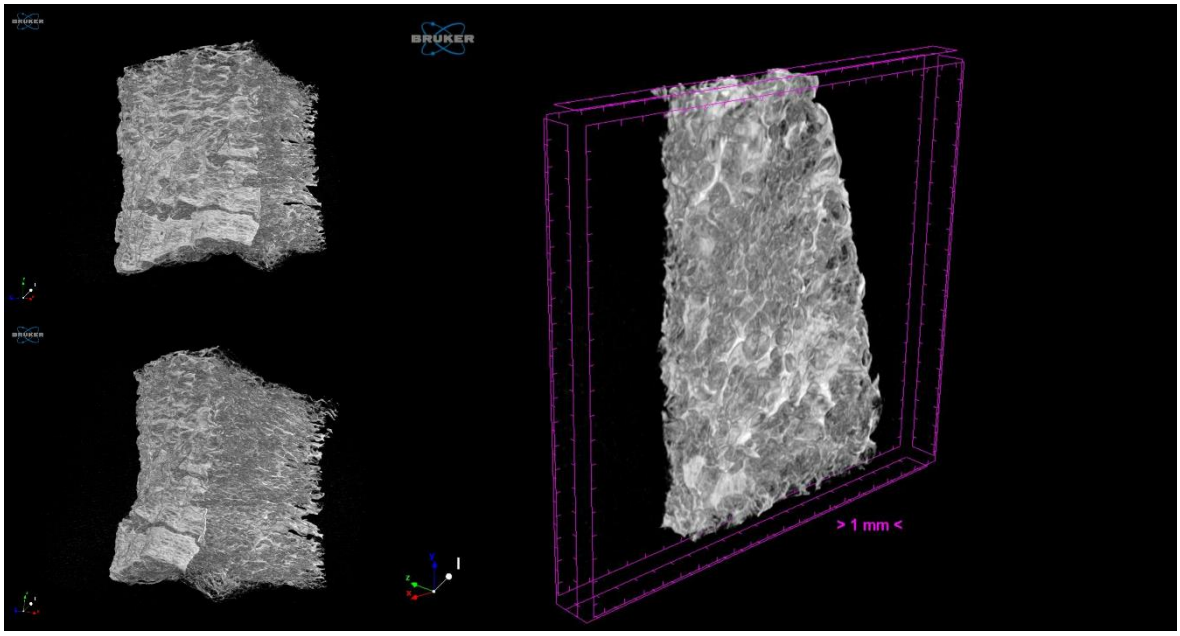


**Figure 4-12 Sample B with 100% infill**

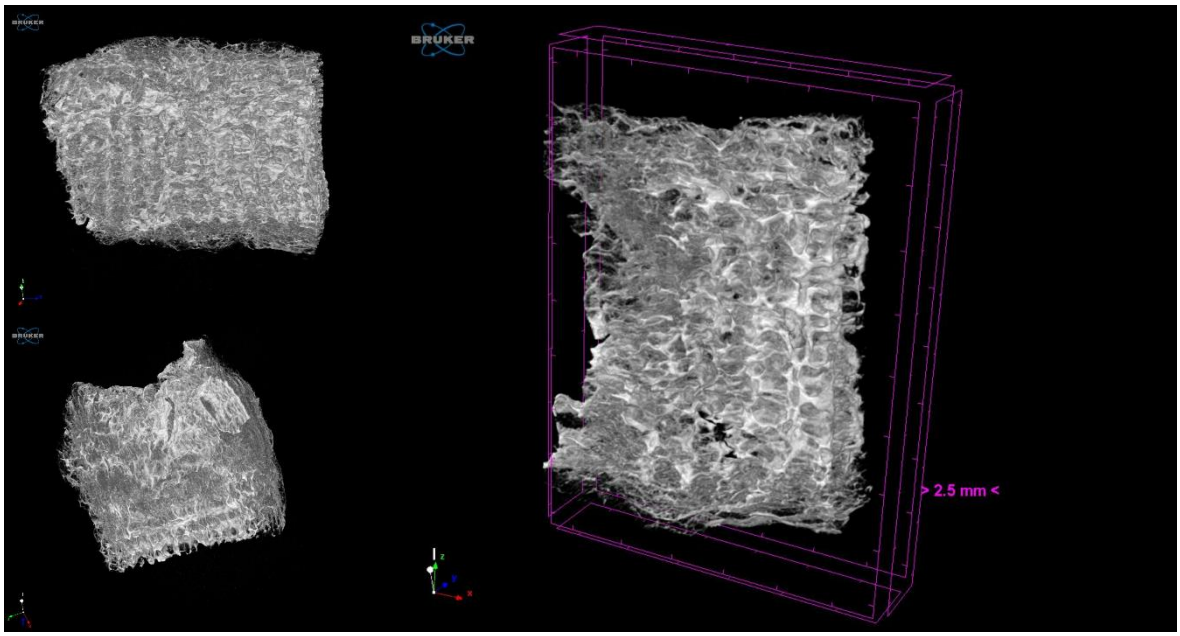


**Figure 4-13 Sample B with 75% infill**

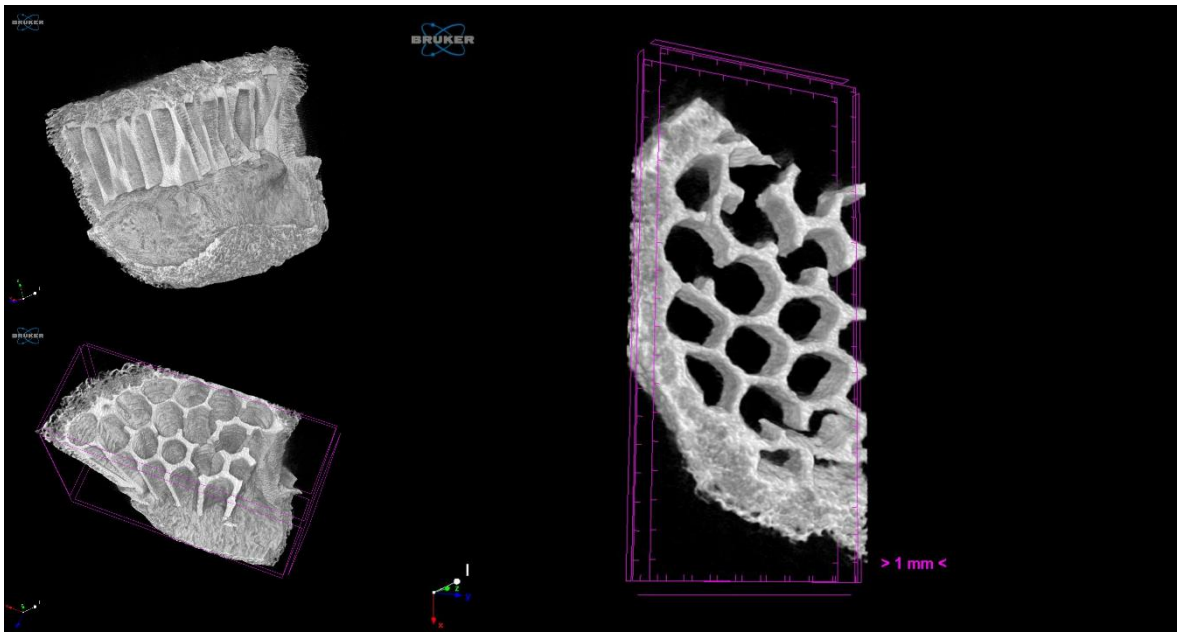


**Figure 4-14 Sample B with 50% infill**

The primary goal of the CT scan was to determine the internal structure of the expanded foams because, as can be seen, the structures with 100% and 75% infill had the highest levels of expansion and the structures with 50% infill had the lowest levels of expansion. Therefore, we performed this procedure to determine the internal structure of the foams because the 50% infill didn't exhibit much expansion.

As shown in the figures above, samples with 100% infill exhibit 77.60% porosity because fewer voids in the sample trapped more air, aiding in the foams expansion when heated in the furnace, while samples with 50% infill exhibit 69.00% porosity because more voids and also more surface area exposed this allowed air to escape through the infill structure, preventing the samples from exhibiting any expansion.

# 5. Conclusions

## 5.1. Conclusions

After researching various additive manufacturing techniques to create foamed structures for the thesis, we came up with the idea of producing the foams using a physical blowing agent. When we conducted the experiment, the results were as expected. Next, we found a research paper that claimed to have produced the foams using a chemical blowing agent. We then attempted to validate their findings.

As we can see in the results that the chemical blowing agent can produce good results as compared to the physical blowing agent, and in chemical blowing agent have the maximum amount of the expansion with the infill with the 100% and then they are being followed by 75% and 50%, as 50% expansion showed us the least amount of expansion. As the expansion of the foams is directly proportional to the infill of the structure, more material in the foams leads to more of the expansions.

We can observe the specimen with 50% of infill's cell structure had not expanded as much as the other specimens', and it was not able to withstand as much stress as the others. As a result, specimens with 100% of infill can withstand greater stress, followed by specimens with 75% because they had more material in the same volume  And the samples with 100% and 75% of infill exhibit the greatest amount of expansion due to the structure formation occurring within their closer-packed cell structures, while the sample with 50% of infill had almost 50% of its internal area of the cells exposed on the results of the CT scan, which prevented the air from being trapped inside the structure and caused the lowest expansion.

## 5.2. Future Works

The future works directions include:

Investigation of sample C, which behaved differently than predicted by the research paper (Wirth et al. 2020), since it was predicted to expand by 750% but only showed 56.18% expansion.

# References

Ahmad, K. W. H., Mohamad, Z., Othman, N., Man, S. H. C., & Jusoh, M. (2020). The mechanical properties of photopolymer prepared via 3d stereolithography printing: The effect of uv curing time and anisotropy. *Chemical Engineering Transactions*, *78*, 565–570. https://doi.org/10.3303/CET2078095

Ali, E. S., & Ahmad, S. (2012). Bio nano composite hybrid polyurethane foam reinforced with empty fruit bunch and nanoclay. *Composites Part B: Engineering*, *43*(7), 2813–2816. https://doi.org/10.1016/j.compositesb.2012.04.043

amfg. (2018). *3D printing with resin: An Introduction*. https://amfg.ai/2018/07/16/3d-printing-resins-introduction/

ASTM, I. (2010). ASTM. In *F2792-10: standard terminology for additive manufacturing technologies. ASTM International.*

Bagheri, A., & Jin, J. (2019). Photopolymerization in 3D Printing. *ACS Applied Polymer Materials*, *1*(4), 593–611. https://doi.org/10.1021/acsapm.8b00165

Balli, J., Kumpaty, S., & Anewenter, V. (2017). Continuous liquid interface production of 3D objects: An unconventional technology and its challenges and opportunities. *ASME International Mechanical Engineering Congress and Exposition . American Society of Mechanical Engineers., 58400*.

Bartolo, P. J. (2011). *Stereolithography: materials, processes and applications*.

Berman, B. (2012). 3-D printing: The new industrial revolution. *Business Horizons*, *55*(2), 155–162. https://doi.org/10.1016/j.bushor.2011.11.003

Castle Island, C. (2009). *How do photopolymer work*.

Cesaretti, G., Dini, E., De Kestelier, X., Colla, V., & Pambaguian, L. (2014). Building components for an outpost on the Lunar soil by means of a novel 3D printing technology. *Acta Astronautica*, *93*, 430–450. https://doi.org/10.1016/j.actaastro.2013.07.034

Chohan, J. S., Singh, R., Boparai, K. S., Penna, R., & Fraternali, F. (2017). Dimensional accuracy analysis of coupled fused deposition modeling and vapour smoothing operations for biomedical applications. *Composites Part B: Engineering*, *117*, 138–149. https://doi.org/10.1016/j.compositesb.2017.02.045

Craveiro, F., Duarte, J. P., Bartolo, H., & Bartolo, P. J. (2019). Additive manufacturing as an enabling technology for digital construction: A perspective on Construction 4.0.

*Automation in Construction*, *103*(October 2018), 251–267. https://doi.org/10.1016/j.autcon.2019.03.011

Dendukuri, D., Panda, P., Haghgooie, R., Kim, J. M., Hatton, T. A., & Doyle, P. S. (2008). Modeling of oxygen-inhibited free radical photopolymerization in a PDMS microfluidic device. *Macromolecules*, *41*(22), 8547–8556. https://doi.org/10.1021/ma801219w

Diptanshu, Young, E., Ma, C., Obeidat, S., Pang, B., & Kang, N. (2018). Ceramic additive manufacturing using vat photopolymerization. *ASME 2018 13th International Manufacturing Science and Engineering Conference, MSEC 2018*, *1*(June). https://doi.org/10.1115/MSEC2018-6389

DUS Architects. (2016). *The Europe Building (The Netherlands)*. https://www.arch2o.com/europe-building-the-eu-presidency-dus-architects/

Fast Radius. (2021). *All about vat photopolymerization*. https://doi.org/https://www.fastradius.com/resources/vat-photopolymerization/

Feixiang, Z., Liyong, Z., & Xia, K. (2016). Study of impact of 3D printing technology and development on creative industry. *Journal of Social Science Studies*, *3*(2), 57. https://doi.org/10.5296/jsss.v3i2.9106

form labs. (2021). *Using draft resin*. https://support.formlabs.com/s/article/Using-Draft-Resin?language=en_US

Galati, M., & Minetola, P. (2020). On the measure of the aesthetic quality of 3D printed plastic parts. *International Journal on Interactive Design and Manufacturing*, *14*(2), 381–392. https://doi.org/10.1007/s12008-019-00627-x

Galjaard, S., Hofman, S., Perry, N., & Ren, S. (2015). Optimizing Structural Building Elements in Metal by using Additive Manufacturing. *Proceedings of the International Association for Shell and Spatial Structures (IASS)*, *August*.

Gama, N., Ferreira, A., & Barros-Timmons, A. (2019). *3D printed cork/polyurethane composite foams*. *179*, 107905. https://doi.org/10.1016/j.matdes.2019.107905

Gama, N., Soares, B., Freire, C. S. R., Silva, R., Ferreira, A., & Barros-Timmons, A. (2018). Effect of unrefined crude glycerol composition on the properties of polyurethane foams. *Journal of Cellular Plastics*, *54*(3), 633–649. https://doi.org/10.1177/0021955X17732304

Gama, N. V., Soares, B., Freire, C. S. R., Silva, R., Neto, C. P., Barros-Timmons, A., & Ferreira, A. (n.d.). Bio-based polyurethane foams toward applications beyond thermal insulation. *Materials and Design*, *76*, 77–85. https://doi.org/10.1016/j.matdes.2015.03.032

Gama, N. V., Soares, B., Freire, C. S., Silva, R., Brandão, I., Neto, C. P., Barros-Timmons, A., & Ferreira, A. (n.d.). Rigid polyurethane foams derived from cork liquefied at atmospheric pressure. *Polymer International*, *64*(2), 250–257. https://doi.org/10.1002/pi.4783

Geisler, C. G. (2011). *Thermosensitive and Photocrosslinkable Composite Polymer study for 3-D Soft Tissue Scaffold Printing* (Issue July).

Haggerty, S., Michael, J., Williams, P. A., & Lawrence, P. E. (1993). *United States Patent (19)*. *19*.

Houbertz, R., Domann, G., Schulz, J., Olsowski, B., Fröhlich, L., & Kim, W. S. (2004). Impact of photoinitiators on the photopolymerization and the optical properties of inorganic-organic hybrid polymers. *Applied Physics Letters*, *84*(7), 1105–1107. https://doi.org/10.1063/1.1647706

IAAC. (2016). *3d-printed-bridge*. https://iaac.net/project/3d-printed-bridge/

Jin, F. L., Zhao, M., Park, M., & Park, S. J. (2019). Recent trends of foaming in polymer processing: A review. In *Polymers* (Vol. 11, Issue 6). https://doi.org/10.3390/polym11060953

Kafara, M., Süchting, M., Kemnitzer, J., Westermann, H. H., & Steinhilper, R. (2017). Comparative Life Cycle Assessment of Conventional and Additive Manufacturing in Mold Core Making for CFRP Production. *Procedia Manufacturing*, *8*(October 2016), 223–230. https://doi.org/10.1016/j.promfg.2017.02.028

Kang, H. W., & Cho, D. W. (2012). Development of an indirect stereolithography technology for scaffold fabrication with a wide range of biomaterial selectivity. *Tissue Engineering - Part C: Methods*, *18*(9), 719–729. https://doi.org/10.1089/ten.tec.2011.0621

Kazemian, A., Yuan, X., Cochran, E., & Khoshnevis, B. (2017). Cementitious materials for construction-scale 3D printing: Laboratory testing of fresh printing mixture. *Construction and Building Materials*, *145*, 639–647. https://doi.org/10.1016/j.conbuildmat.2017.04.015

Kruth, J. P., Leu, M. C., & Nakagawa, T. (1998). Progress in additive manufacturing and rapid prototyping. *CIRP Annals - Manufacturing Technology*, *47*(2), 525–540. https://doi.org/10.1016/S0007-8506(07)63240-5

Lee, C. H., Lee, K. J., Jeong, H. G., & Kim, S. W. (2000). Growth of gas bubbles in the foam extrusion process. *Advances in Polymer Technology*, *19*(2), 97–112. https://doi.org/10.1002/(SICI)1098-2329(200022)19:2<97::AID-ADV3>3.0.CO;2-B

Li, M., Chen, Y., Zhang, H., & Wang, T. (2010). A novel ferrocenium salt as visible light photoinitiator for cationic and radical photopolymerization. *Progress in Organic Coatings*, *68*(3), 234–239. https://doi.org/10.1016/j.porgcoat.2010.01.007

Lim, C. W. J., Le, K. Q., Lu, Q., & Wong, C. H. (2016). An Overview of 3-D Printing in Manufacturing, Aerospace, and Automotive Industries. *IEEE Potentials*, *35*(4), 18–22. https://doi.org/10.1109/MPOT.2016.2540098

Long, Y., An, J., & Xie, X. (2020). CO2-releasing blowing agents from modified polyethylenimines slightly consume isocyanate groups while foaming polyurethanes.

*Arabian Journal of Chemistry*, *13*(1), 3226–3235. https://doi.org/10.1016/j.arabjc.2018.10.007

Lovo, J. F. P., de Camargo, I. L., Erbereli, R., Morais, M. M., & Fortulan, C. A. (2020). Vat photopolymerization additive manufacturing resins: Analysis and case study. *Materials Research*, *23*(4), 1–10. https://doi.org/10.1590/1980-5373-MR-2020-0010

Ma, G., & Wang, L. (2018). A critical review of preparation design and workability measurement of concrete material for largescale 3D printing. *Frontiers of Structural and Civil Engineering*, *12*(3), 382–400.

Medellin, A., Du, W., Miao, G., Zou, J., Pei, Z., & Ma, C. (2019). Vat photopolymerization 3d printing of nanocomposites: A literature review. *Journal of Micro and Nano-Manufacturing*, *7*(3). https://doi.org/10.1115/1.4044288

Melchels, F. P. W., Feijen, J., & Grijpma, D. W. (2010). A review on stereolithography and its applications in biomedical engineering. *Biomaterials*, *31*(24), 6121–6130. https://doi.org/10.1016/j.biomaterials.2010.04.050

Mireles, J., Espalin, D., Roberson, D., Zinniel, B., Medina, F., & Wicker, R. (2012). Fused deposition modeling of metals. *23rd Annual International Solid Freeform Fabrication Symposium - An Additive Manufacturing Conference, SFF 2012*, 836–845.

Mohamed, O. A., Masood, S. H., & Bhowmik, J. L. (2015). Optimization of fused deposition modeling process parameters: a review of current research and future prospects. *Advances in Manufacturing*, *3*(1), 42–53. https://doi.org/10.1007/s40436-014-0097-7

Mukhametov, R. R., Merkulova, Y. I., & Chursova, L. V. (2012). Thermoreactive polymer binders with a predicted level of rheological and deformation properties. *Polymer Science - Series D*, *5*(4), 261–263. https://doi.org/10.1134/S1995421212040119

Nik Pauzi, N. N. P., Majid, R., Dzulkifli, M. H., & Yahya, M. Y. (2014). Development of rigid bio-based polyurethane foam reinforced with nanoclay. *Composites Part B: Engineering*, *67*, 521–526. https://doi.org/10.1016/j.compositesb.2014.08.004

Pacewicz, K., Sobotka, A., & Gołek, Ł. (2018). Characteristic of materials for the 3D printed building constructions by additive printing. *MATEC Web of Conferences*, *01013*.

Pagac, M., Hajnys, J., Ma, Q. P., Jancar, L., Jansa, J., Stefek, P., & Mesicek, J. (2021). A review of vat photopolymerization technology: Materials, applications, challenges, and future trends of 3d printing. *Polymers*, *13*(4), 1–20. https://doi.org/10.3390/polym13040598

Patil, B., Bharath Kumar, B. R., & Doddamani, M. (2019). Compressive behavior of fly ash based 3D printed syntactic foam composite. *Materials Letters*, *254*, 246–249. https://doi.org/10.1016/j.matlet.2019.07.080

Pham, D. T., & Gault, R. S. (1998). A comparison of rapid prototyping technologies. *International Journal of Machine Tools and Manufacture*, *38*(10–11), 1257–1287. https://doi.org/10.1016/S0890-6955(97)00137-5

PrintWiki. (2013). *Printwiki, (2013). Photopolymer. [Online] Available at: http://printwiki.org/Photopolymer. [*. PrintWiki.

Printwiki. (2021). *Photopolymer*. Printwiki. http://printwiki.org/Polymerization

Quan, H., Zhang, T., Xu, H., Luo, S., Nie, J., & Zhu, X. (2020). Photo-curing 3D printing technique and its challenges. *Bioactive Materials*, *5*(1), 110–115. https://doi.org/10.1016/j.bioactmat.2019.12.003

Salamone, J. C. (1996). *Polymeric Materials Encyclopedia*.

Sambu, S., Chen, Y., & Rosen, D. W. (2004). Geometric tailoring: A design for manufacturing method for rapid prototyping and rapid tooling. *Journal of Mechanical Design, Transactions of the ASME*, *126*(4), 571–580. https://doi.org/10.1115/1.1758250

Schlögl, S., Reischl, M., Ribitsch, V., & Kern, W. (2012). UV induced microcellular foaming - A new approach towards the production of 3D structures in offset printing techniques. *Progress in Organic Coatings*, *73*(1), 54–61. https://doi.org/10.1016/j.porgcoat.2011.08.020

Sing, S. L., An, J., Yeong, W. Y., & Wiria, F. E. (2016). Laser and electron-beam powder-bed additive manufacturing of metallic implants: A review on processes, materials and designs. *Journal of Orthopaedic Research*, *34*(3), 369–385. https://doi.org/10.1002/jor.23075

Slapnik, J., Stiller, T., Wilhelm, T., & Hausberger, A. (2020). Influence of solid lubricants on the tribological performance of photocurable resins for vat photopolymerization. *Lubricants*, *8*(12), 1–19. https://doi.org/10.3390/lubricants8120104

Song, W., Barber, K., & Lee, K. Y. (2017). Heat-induced bubble expansion as a route to increase the porosity of foam-templated bio-based macroporous polymers. *Polymer*, *118*, 97–106. https://doi.org/10.1016/j.polymer.2017.04.058

Sood, A. K., Ohdar, R. K., & Mahapatra, S. S. (2010). Parametric appraisal of mechanical property of fused deposition modelling processed parts. *Materials and Design*, *31*(1), 287–295. https://doi.org/10.1016/j.matdes.2009.06.016

Sun, L., & Zhao, L. (2017). Envisioning the era of 3D printing: a conceptual model for the fashion industry. *Fashion and Textiles*, *4*(1). https://doi.org/10.1186/s40691-017-0110-4

Taormina, G., Sciancalepore, C., Messori, M., & Bondioli, F. (2018). 3D printing processes for photocurable polymeric materials: technologies, materials, and future trends. *Journal of Applied Biomaterials and Functional Materials*, *16*(3), 151–160. https://doi.org/10.1177/2280800018764770

Torabi, K., Farjood, E., & Hamedani, S. (2015). *Rapid Prototyping Technologies and their Applications in Prosthodontics , a Review of Literature*. *16*(March), 1–9.

Tsuchida, E., Nishide, H., Yamamoto, K., & Yoshida, S. (1987). Electrooxidative polymerization of thiophenol to yield poly (p-phenylene sulfide). *Macromolecules*.

Utela, B., Storti, D., Anderson, R., & Ganter, M. (2008). A review of process development steps for new material systems in three dimensional printing (3DP). *Journal of Manufacturing Processes*, *10*(2), 96–104. https://doi.org/10.1016/j.jmapro.2009.03.002

Wang, X., Jiang, M., Zhou, Z., Gou, J., & Hui, D. (2017a). 3D printing of polymer matrix composites: A review and prospective. *Composites Part B: Engineering*, *110*, 442–458. https://doi.org/10.1016/j.compositesb.2016.11.034

Wang, X., Jiang, M., Zhou, Z., Gou, J., & Hui, D. (2017b). 3D printing of polymer matrix composites: A review and prospective. *Composites Part B: Engineering*, *110*, 442–458. https://doi.org/10.1016/j.compositesb.2016.11.034

William Reusch. (2020). *Polymers and Polymerization Reactions*. Virtual Text Book of Chemistry. https://chem.libretexts.org/@go/page/24397

Wirth, D. M., Jaquez, A., Gandarilla, S., Hochberg, J. D., Church, D. C., & Pokorski, J. K. (2020). Highly Expandable Foam for Lithographic 3D Printing. *ACS Applied Materials and Interfaces*, *12*(16), 19033–19043. https://doi.org/10.1021/acsami.0c02683

Yan, Q., Dong, H., Su, J., Han, J., Song, B., Wei, Q., & Shi, Y. (2018). A Review of 3D Printing Technology for Medical Applications. *Engineering*, *4*(5), 729–742. https://doi.org/10.1016/j.eng.2018.07.021

Zhang, G., Wang, B., Ma, L., Wu, L., Pan, S., & Yang, J. (2014). Energy absorption and low velocity impact response of polyurethane foam filled pyramidal lattice core sandwich panels. *Composite Structures*, *108*(1), 304–310. https://doi.org/10.1016/j.compstruct.2013.09.040

Zhao, C., Fezzaa, K., Cunningham, R. W., Wen, H., De Carlo, F., Chen, L., Rollett, A. D., & Sun, T. (2017). Real-time monitoring of laser powder bed fusion process using high-speed X-ray imaging and diffraction. *Scientific Reports*, *7*(1), 1–11. https://doi.org/10.1038/s41598-017-03761-2